Received: 12 May 2025 | Revised: 27 August 2025 | Accepted: 24 November 2025

DOI: 10.1002/dep2.70058

The Depositional Record Open Access
A journal of the International Association of Sedimentologists
WILEY

ORIGINAL ARTICLE

Microbial mediation and climatic control on dolomite precipitation in a hypersaline lake: Insights from Salinas Lake, southern Iberia

Guolai Li[1] | **Zeina Naim**[1] | **Luis Gibert**[2] | **Jan-Berend Stuut**[1,3] | **Annemiek C. Waajen**[1] | **Gonzalo Jimenez-Moreno**[4] | **Mónica Sánchez-Román**[1,5]

[1]Earth Sciences Department, Faculty of Science, Vrije Universiteit Amsterdam, Amsterdam, The Netherlands

[2]Mineralogy, Petrology and Applied Geology Department, University of Barcelona, Barcelona, Spain

[3]Department of Ocean Systems, NIOZ Royal-Netherlands Institute for Sea Research, Den Burg, The Netherlands

[4]Stratigraphy and Paleontology Department, Sciences Faculty, University of Granada, Granada, Spain

[5]Mineralogy and Petrology Department, Sciences Faculty, University of Granada, Granada, Spain

Correspondence
Guolai Li and Mónica Sánchez-Román, Earth Sciences Department, Faculty of Science, Vrije Universiteit Amsterdam, 1081HZ Amsterdam, The Netherlands.
Email: l.g.l.li@vu.nl; m.sanchezroman@ugr.es

Funding information
Nederlandse Organisatie voor Wetenschappelijk Onderzoek, Grant/Award Number: OCENW.KLEIN.037 and ENW.GO.001.033

Abstract

This study examines the climatic controls on dolomite precipitation through a multiproxy investigation of a carbonate-rich sediment core from Salinas Lake, a hypersaline playa in Alicante, south-eastern Iberia. The ~120,000 year record captures depositional cycles and palaeoenvironmental changes driven by late Pleistocene to Holocene climate variability. Integrated analyses of sedimentology, lithology, geochemistry (elemental concentrations, total organic carbon, stable carbon and oxygen isotopes), scanning electron microscopy, microbial community characterisation and palynology reconstruct lake hydrology and its influence on carbonate mineralogy. The sediment succession is marked by alternating calcite- and dolomite-rich intervals, with dolomite crystals displaying morphological evolution from spherical to rhombohedral forms with depth. Stable isotope signatures ($\delta^{13}C$: −6.5‰ to −2.4‰ VPDB; $\delta^{18}O$: −2.3‰ to +4.9‰ VPDB), alongside microbial structures such as extracellular polymeric substances (EPS) and internal crystal voids, suggest a biologically mediated precipitation mechanism. These mineralogical shifts closely correspond to rapid hydrological changes driven by Dansgaard–Oeschger climate oscillations, with dolomite formation favoured under arid, evaporative conditions that concentrate Mg and Ca ions and promote microbial mat development. Halophilic microbial communities, capable of catalysing carbonate precipitation, probably enhance dolomite nucleation and growth through EPS production and geochemical modulation. This work underscores the complex interplay between climate, hydrology, microbial activity and sedimentary mineral formation, providing new insights into the longstanding 'dolomite problem' within sedimentary environments.

KEYWORDS

bacteria, geochemistry, lacustrine dolomite, paleoclimate, stable isotopes

1 | INTRODUCTION

Dolomite, [$CaMg(CO_3)_2$], a common carbonate mineral, serves as a valuable archive of past environmental conditions, providing insights into depositional settings and paleoclimate dynamics (Guo, Wen, Li, et al., 2023; Mueller et al., 2022; Naim et al., 2025; Sánchez-Román, McKenzie, et al., 2011; Sánchez-Román et al., 2023; Zhao et al., 2023; Yao et al., 2024). This is especially critical in evaporitic playa-lake systems, which are highly sensitive to climatic fluctuations and capable of recording even subtle environmental changes (Battarbee, 2000; García-Alix et al., 2022; Giralt et al., 2008; McCormack et al., 2024; Sánchez-Román et al., 2023). However, despite its widespread occurrence in the geological record, the mechanisms controlling dolomite precipitation remain a long-standing question in sedimentary geology, often referred to as the 'dolomite problem' (Liu, Fan, et al., 2020; Liu, Xu, et al., 2020; McKenzie & Vasconcelos, 2009; Sánchez-Román et al., 2008, 2009; Warren, 2000), as modern dolomite formation is rare and synthesising dolomite under ambient Earth-surface temperatures in laboratory settings remains challenging.

Contemporary saline and evaporitic lacustrine environments provide important natural laboratories for investigating dolomite precipitation processes under low-temperature conditions. In these settings, dolomite frequently occurs alongside microbial structures such as microbial mats, bacterial cells, biofilms and extracellular polymeric substance (EPS) (Bontognali et al., 2010; Brauchli et al., 2016; Deng et al., 2010; Sánchez-Román et al., 2008, 2009; Vasconcelos & McKenzie, 1997; Wright & Wacey, 2005). Experimental and field studies indicate that the kinetic barrier to dolomite formation, largely associated with the strong hydration shell of Mg^{2+} ions, is generally overcome only at elevated temperatures (>100°C) (Lippmann, 1973; Miller et al., 2018; Power et al., 2017). However, numerous studies have shown that microbial activity and associated EPSs can facilitate dolomite precipitation at low temperatures by helping to overcome this kinetic barrier (e.g. Fang et al., 2023; Roberts et al., 2013; Sánchez-Román et al., 2025). Consequently, considerable research has focused on identifying catalysts that could facilitate dolomite precipitation at low temperatures (<50°C), with microbial mediation emerging as a key mechanism (Chen et al., 2024; Daye et al., 2019; Deng et al., 2010; Liu, Yu, et al., 2019; Sánchez-Román et al., 2025; Sánchez-Román, McKenzie, et al., 2011; Sánchez-Román, Romanek, et al., 2011; van Lith et al., 2003; Wright, 1999). Microorganisms can promote carbonate mineralisation by modifying local geochemical conditions, such as pH, alkalinity and Mg/Ca ratios, and by providing nucleation sites for crystal growth (Sanchez-Roman et al., 2015, 2014, 2025; McKenzie, et al., 2011; Sánchez-Román, Romanek, et al., 2011; van Lith et al., 2003). Nevertheless, the precise microbial pathways leading to dolomite precipitation remain incompletely understood.

Beyond microbial mediation, recent research suggests that abiotic processes may also facilitate dolomite formation, with clay minerals serving as catalysts by supplying Mg^{2+} and offering nucleation surfaces (Fang et al., 2023; Guo, Wen, & Sánchez-Román,2023; Liu, Xu, et al., 2019; Wanas & Sallam, 2016; Wen et al., 2020). Thus, dolomite precipitation in natural environments may be governed by a complex interplay of biological and abiotic mechanisms. Disentangling these contributions remains a significant challenge, particularly in modern environments where dolomite formation is sporadic and highly sensitive to variable geochemical conditions.

The lacustrine systems of south-eastern Iberia, notably the shallow, saline, endorheic lakes, offer a unique opportunity to investigate dolomite formation processes. These lakes, characterised by carbonate-rich Quaternary sediments (e.g. García-Alix et al., 2022; Valero-Garcés et al., 2014), provide valuable contemporary analogues for studying dolomite formation under the Earth's surface conditions. Among them, Salinas Lake is especially noteworthy, as the occurance of dolomite precipitation is still active there under present-day conditions (Queralt et al., 1997). While previous research has primarily focused on reconstructing lake hydrology and palaeoenvironmental changes using pollen and fossil assemblages (Burjachs et al., 2016; Giralt et al., 1999; Roca & Juliá, 1997), a comprehensive mineralogical, geochemical and petrographic analysis of the lake's dolomitic sediments remains lacking.

To address this gap, a new sediment core was retrieved from Salinas Lake and analysed using a multiproxy approach that integrates mineralogical (XRD), geochemical (XRF, stable isotopes, C/N ratios), microbiological and electron microscopy techniques alongside existing palynological data. This study aims to (i) characterise the mineralogical, geochemical and petrographic features of modern dolomite in Salinas Lake and (ii) evaluate the environmental controls and potential microbial or abiotic mechanisms governing its precipitation. Through this approach, the study seeks to advance understanding of low-temperature dolomite formation, with broader implications for palaeoenvironmental reconstructions and carbonate sedimentology.

2 | GEOLOGICAL SETTINGS

Salinas Lake (38°30′ N 0°53′ W) is an ephemeral lake located near Salinas, Alicante, Spain (Figure 1), with a

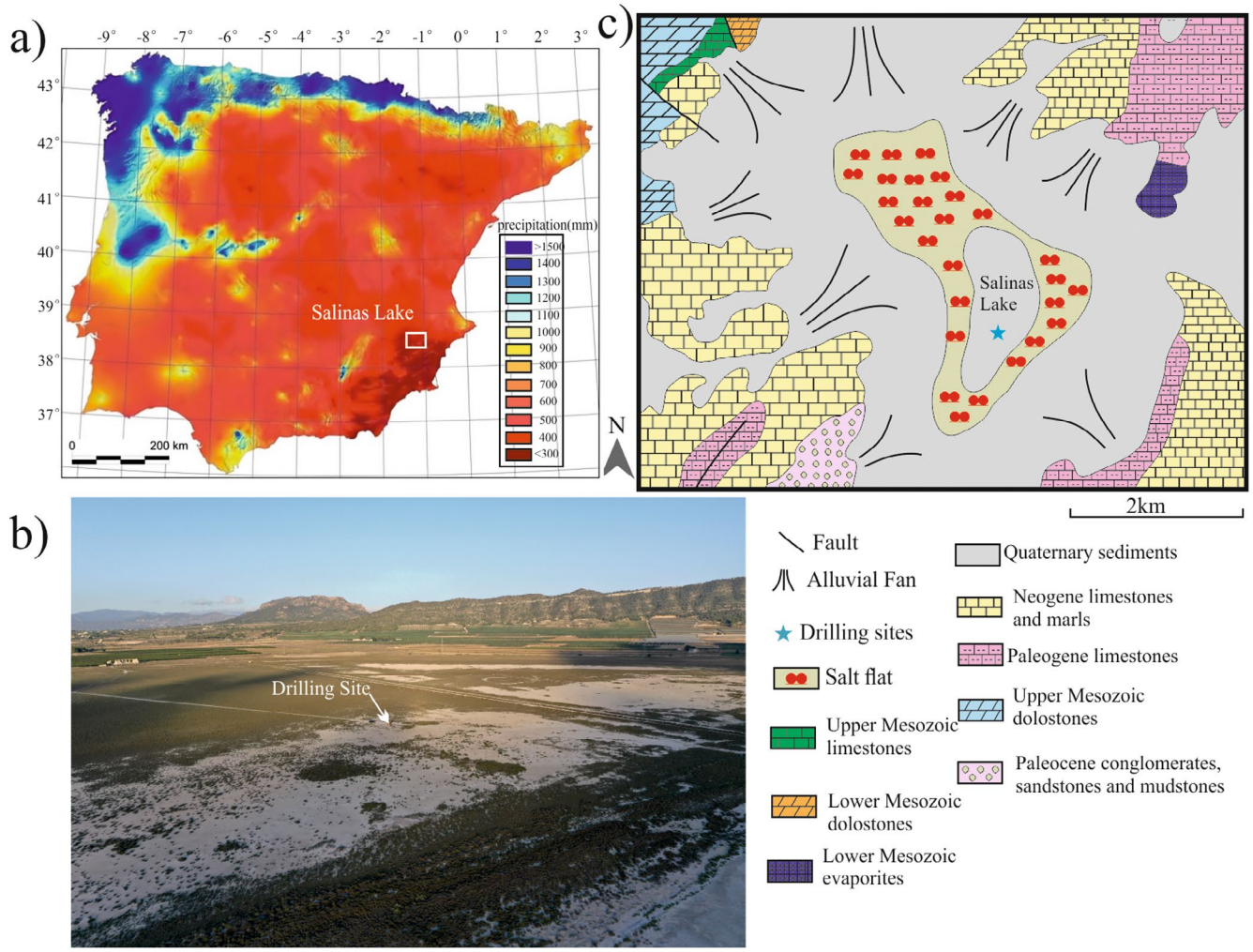

FIGURE 1 Geological and hydrological setting of Salinas Lake. (A) Annual precipitation map of the Iberian Peninsula (Ninyerola et al., 2005). (B) Overhead view of Salinas Lake. (C) Geographic location of Salinas Lake. The annual precipitation in Alicante is <400 mm, making Salinas Lake an ephemeral system that only refills during the rainy season. The lake is situated on a salt flat and is covered by Quaternary sediments, surrounded by mountain ranges composed primarily of Tertiary and Mesozoic limestones and dolostones.

surface area of approximately 1.6 km^2 and a catchment area of about 71 km^2 (Giralt et al., 1999). Situated at the terminus of the Eastern Alpine Betic Chain, it lies roughly 40 km north-west of Alicante, at an elevation of 475 m. To the north-west, the Serra de les Salinas mountain range reaches a maximum height of 1240 m above sea level and is primarily composed of Mesozoic limestone and dolostone units. To the south-east, another mountain range consists mainly of Neogene limestone. The northern region features outcrops of the Triassic Keuper Formation, which includes gypsum-bearing sediments. Between the lake and these mountain ranges, large alluvial fans and detrital slope debris have accumulated. The lake occupies an endorheic basin separated by a threshold that is 40–50 m above the lake surface. If breached, this threshold could lead to the lake transitioning into an open system through overflooding.

Historically, Salinas Lake was replenished by run-off and groundwater, with an annual mean precipitation of 350 mm and high annual evapotranspiration rates of 1500 mm (Ninyerola et al., 2005; Pepiol-Salom et al., 1999). However, extensive groundwater extraction over recent centuries has resulted in a significant decline in water levels, transforming the lake into a playa system (shallow and ephemeral saline lake generally developed in arid/semi-arid regions) that refills only during rainy seasons. The lake water is slightly alkaline, with a pH of approximately 7.5, and is dominated by cations such as Na^+, Mg^{2+} and Ca^{2+}, as well as anions like SO_4^{2-} and Cl^- (Giralt, 1998). This chemical environment supports halophytic vegetation. Today, Salinas Lake is characterised by a landscape of open and shrub vegetation, with sparse woodland on the surrounding hills. The predominant tree species include *Quercus ilex*, *Pinus halepensis*, *Pinus pinea*, *Pinus pinaster* and *Rhamnus oleoides*, while

shrub species include *Quercus coccifera*, *Juniperus oxycedrus*, *Juniperus phoenicea*, *Pistacia terebinthus*, *Daphne gnidium*, *Rosmarinus officinalis*, *Thymus vulgaris*, *Stipa tenacissima* and *Tetraclinis articulata*, an endemic species (Burjachs et al., 2016; Rigual, 1972).

3 | MATERIALS AND METHODS

3.1 | Sediment cores

In July 2021, a 31 m long sediment core (38°30′11″ N 0°53′12″ W) was extracted from Salinas Lake in Alicante, Spain, using a Rotalec drill operated by the Centro de Instrumentación Científica (CIC) at the Universidad de Granada. Upon retrieval, the core sections were stored in a refrigerated room at 4°C to preserve their integrity until further processing. The core was opened, described based on lithological characteristics and photographed prior to sampling.

3.2 | Mineralogy

In total, 66 sediment samples (~1 cm^3) were collected along the core for mineralogical analysis. After sampling, the sediments were dried and ground into a fine powder. Mineralogical composition was determined using X-ray diffraction (XRD) with a Bruker-AXS D8 ADVANCE diffractometer (DAVINCI design) equipped with an LYNXEYE XE-T detector at the GEO3BCN-CSIC laboratory of Barcelona University, Spain. The analysis was conducted over a 2θ range from 2° to 75° at a scanning speed of 2° min^{-1}. Mineral identification was performed using the Panalytical HighScore software package, and relative mineral abundances were estimated based on peak intensities.

3.3 | X-ray fluorescence (XRF) core scanner

Elemental composition was assessed using an X-ray fluorescence (XRF) core scanner. The entire core was scanned with an Avaatech XRF Core Scanner at the Royal Netherlands Institute for Sea Research (NIOZ, the Netherlands). Light elements (e.g. Mg, Al) were analysed with an X-ray current of 0.5 mA/10 kV, while heavy elements (e.g. Mn, Ti) were analysed at 0.25 mA/30 kV, both at a 15-second count time under an argon atmosphere. The raw data, expressed as element intensities (counts per second), were processed statistically using principal component analysis (PCA) and correlation matrix in Origin 2021 software.

3.4 | Total organic carbon and nitrogen

Total organic carbon (TOC) and total nitrogen (TN) were analysed using a Thermo Finnigan CNS Elemental Analyser at the Sediment Laboratory of Vrije Universiteit Amsterdam, the Netherlands. Thirty-six samples were finely ground into a powder, and inorganic carbonate was removed by exposure to a HCl atmosphere. Following this treatment, the remaining material gets combusted and the produced gases will be collected and analysed for TOC and TN determination, with a precision <5% on ~10 mg of material.

3.5 | Stable C and O isotope

$\delta^{18}O$ and $\delta^{13}C$ of 54 dolomite samples were measured at the Stable Isotope Laboratory at the Vrije Universiteit Amsterdam, The Netherlands. Samples containing both calcite and dolomite were digested with EDTA solution (following the process of Geske et al., 2015) to remove the calcite first. Afterwards, samples were also washed with milli-Q water to remove the residue of EDTA that might influence the results. Calcite-free samples were powdered and pre-washed with Milli-Q water to remove any possible salts. Then, these samples were treated with 100% phosphoric acid under vacuum conditions to release CO_2, which was then analysed using Thermo Finnigan Isotope Ratio Mass Spectrometers (IRMS) at 45°C. All $\delta^{18}O$ and $\delta^{13}C$ values are reported in per mil relative to VPDB. The referred carbonate standard, IAEA-603, yielded average results of 2.51‰ (SD 0.13) for $\delta^{13}C$ and −2.31‰ (SD 0.05) for $\delta^{18}O$.

3.6 | Scanning electron microscopy

Sediment observations were carried out by scanning electron microscopy (SEM) coupled with energy-dispersive X-ray spectroscopy (EDS) on a Zeiss Gemini 450 of Electron Microscopy Centre at Utrecht University, the Netherlands. Samples were coated with platinum (Pt) before observation. The instrument operated under a high vacuum environment with an accelerating voltage of 10 kV and a probe current of 300 pA.

3.7 | Radiocarbon age and chronology

The radiocarbon age of nine sediment samples was obtained using accelerator mass spectrometry (AMS) radiocarbon dating at the Poznan Radiocarbon Laboratory, Adam Mickiewicz University, Poznań. Prior to AMS

measurement, samples were treated with HCl to remove inorganic carbon. The carbon was then extracted as CO_2 through combustion, transferred to graphite and analysed via AMS ^{14}C measurements. The age model was constructed using the software Undatable (Lougheed & Obrochta, 2019), with IntCal20 calibration. All samples were included in the bootstrapping process, and the top of the core was assumed to correspond to the present (0 cal yr. BP, i.e. 1950 CE, at 0 m).

3.8 | Pollen analysis

Palynomorph extraction followed a modified version of Faegri and Iversen's methodology (Faegri et al., 1989). Pollen counting was performed under magnifications of ×400 and ×1000, with a minimum of 300 terrestrial pollen grains counted per sample. Fossil pollen was identified by comparing it to modern-day counterparts using published identification keys (Beug, 2004) and a modern pollen reference collection housed at the University of Granada, Spain.

Pollen counts were converted into percentages, excluding aquatic taxa, and a xerophyte group of cold/arid pollen taxa (e.g. *Artemisia* and *Ephedra*) was identified to differentiate between warm/humid and cold/arid phases. The percentage of total *Quercus* (including evergreen and deciduous *Quercus*) was also calculated, which has been previously shown to increase with temperature and precipitation in the study area (Camuera et al., 2019).

3.9 | Microbial communities

DNA of sediment samples and a negative control was extracted and concentrated using the DNeasy PowerMax Soil Kit (QIAGEN GmbH, Germany) with small adjustments to the protocol (details in the supplemental material). Extracted DNA was stored at −20°C and shipped on dry ice to BGI Tech Solutions (HongKong) for amplicon sequencing of the V4 region of the 16S rRNA gene using Illumina MiSeq. FASTQ files from BGI Tech Solutions were analysed using the EDGE Bioinformatics web-based platform which uses automated scripts of QIIME2 version 2023.5.1 (Bokulich et al., 2018; Bolyen et al., 2019; Katoh et al., 2002; Li et al., 2017; Price et al., 2009; Rognes et al., 2016). Operational taxonomic units (OTUs) were binned at a 97% sequence similarity, and a community composition barplot was constructed from the rarefied OTU table. More details can be found in the Supporting Information.

4 | RESULTS

4.1 | Sedimentology and mineralogy

The sediment core from Salinas Lake is described based on its lithological characteristics and X-ray diffraction (XRD) results, shown in Figure 2. A total of 24 distinct sedimentary units were identified, based on the integration of the sedimentological observations and XRD analysis (detailed photographs and descriptions are available in the Supporting Information). The uppermost 60 cm (but only ~20 cm thick sediment core was retrieved) consists of a soil layer containing plant remains, predominantly grass. Beneath this, unaltered sediment is present.

Overall, the core is primarily composed of carbonates, with more than 80% of the composition being carbonate rich. A clear alternation is observed between calcite-dominant (~50% or greater) and dolomite-dominant sediment layers with minor magnesite content (5%, see Supporting Information). The dolomite-rich layers are located approximately at depths of 1 m, 3.5–9.5 m, 12–16 m, 19–21 m, 25–27 m and below 29.5 m. These layers are devoid of calcite, while the calcite-rich layers still contain a small amount of dolomite, typically around 20%. The mineralogy and X-ray fluorescence (XRF) Mg/Ca ratio show a clear correlation, with the dolomite-rich intervals matching the higher Mg/Ca ratios (Figure 2).

4.2 | Chronology

The radiocarbon (AMS ^{14}C) results of nine sediment samples are provided in Table 1. The lower portion of the core (after ~22 m) yields dates that conflict with dates from the upper part, potentially due to contamination or limitations in AMS ^{14}C dating, particularly for ages beyond 50,000 years. Consequently, the bottom dates were excluded from the age model.

As shown in the established age model (Figure 3), the upper ~22 m of Salinas core spans approximately 45–2.5 cal ka BP with uncertainty reaching up to ~3000 years. The boundary between the Holocene and Pleistocene is located at approximately 3.5 m, where a significant change in lithology occurs (from Unit 4b to Unit 4a). The last glacial maximum probably corresponds to the depth range of 7–9 m (Unit 5), characterised by dry and compact dolomitic mud sediment. This is consistent with previous studies (Burjachs et al., 2016; Giralt et al., 1998, 1999) which also reported the Holocene/Pleistocene boundary at around 4 m and the LGM at around 8 m, validating the established age model of our research.

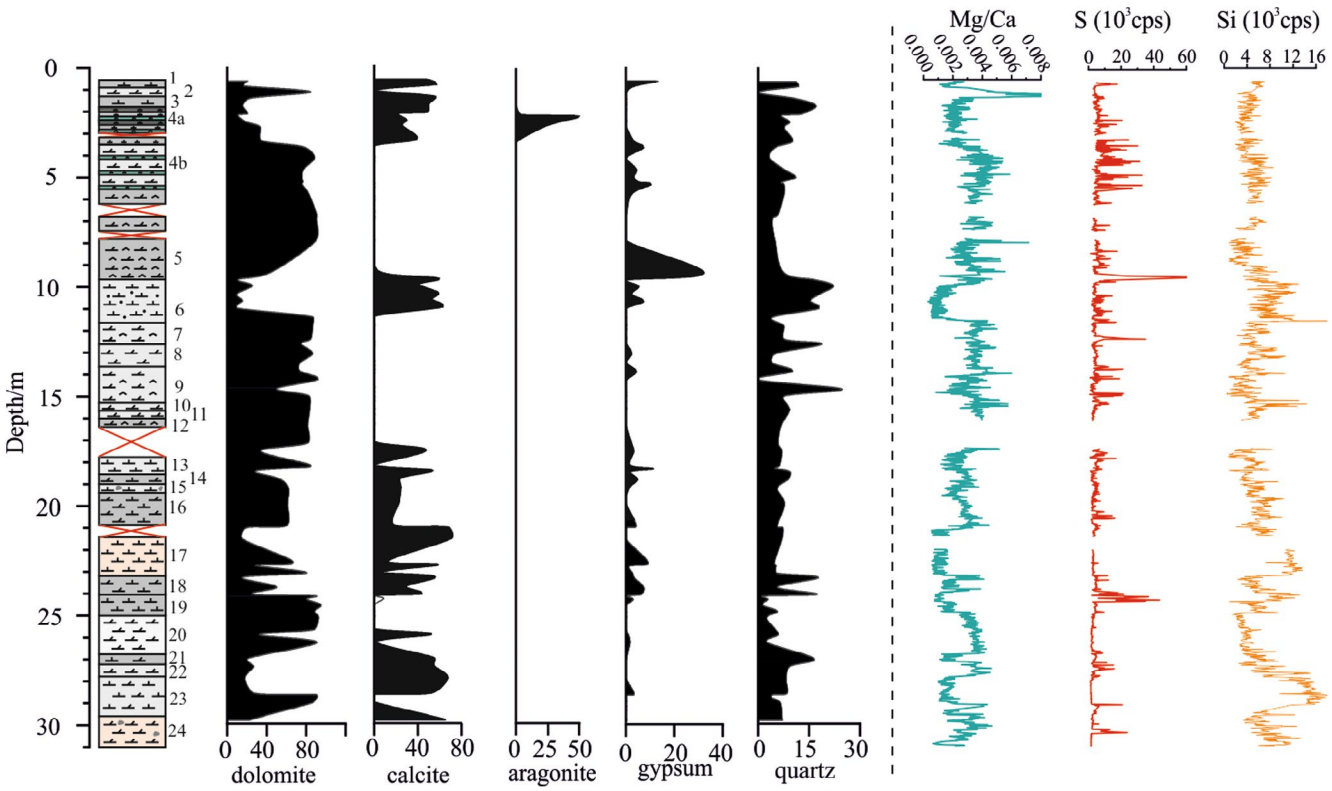

FIGURE 2 Lithology and mineralogy of the Salinas sediment core. The core's lithology and mineralogy, including dolomite, calcite, aragonite, gypsum, and quartz, were determined through XRD analysis. The XRD results are compared with XRF scanning data for Mg/Ca, S and Si, which represent dolomite, gypsum and quartz, respectively. The consistency between the XRF and XRD results validates the reliability of these data.

For the bottom section of Salinas core, a previous palaeomagnetic study (Julià et al., 1994) identified a magnetic reversal at around 30 m depth, originally attributed to the Matuyama–Brunhes reversal at 773 cal ka BP. However, considering the ^{14}C dates and sedimentation rate in Salinas Lake, the Blake Event (~120 ka) (Singer et al., 2014) instead of the Matuyama–Brunhes reversal is a more plausible interpretation and therefore proposed here. While this research did not conduct new palaeomagnetic analysis, the core's similarity to the previously studied sequence (Figure S1) suggests that this reversal may also be present in our core. Based on this, Salinas core spans from approximately 120 cal ka BP to 2.5 cal ka BP, with the Pleistocene–Holocene boundary positioned near 3.5 m.

4.3 | Major and minor elements

The elemental concentrations of the sediment core were analysed using XRF, and the results show a strong correlation between XRD and XRF data (Figure 2). Peaks in the Mg/Ca ratio from XRF correspond closely with the dolomite-rich layers observed in the XRD data. This consistent correlation supports the use of the XRF core scanner as an effective tool for reconstructing high-resolution trends in elemental composition.

Principal component analysis (PCA) and correlation matrix analysis were performed on nine key elements (Mg/Ca ratio, Al, Si, K, Rb, Sr., Fe, Mn and S) (Figure 4). The results reveal a strong positive correlation among six elements (Fe, Mn, K, Ti, Si and Al) indicating that these elements are associated with siliciclastic input. Conversely, Mg/Ca, which primarily indicates dolomite, exhibits a moderate negative correlation with these siliciclastic elements. Sulphur (S), representing gypsum and an evaporative environment, is negatively correlated with the siliciclastic group. PCA shows that principal component 1 (PC1) explains 54.9% of the variance, with the siliciclastic group contributing positively and the evaporative minerals (dolomite and gypsum) contributing negatively. Therefore, PC1 can serve as a proxy for run-off input.

Consistent with PCA results, the plots of Mg/Ca and S show opposite trends with siliciclastic group elements and PC1 (Figure 5). In the dolomite-rich part, the Mg/Ca is higher, and S is more abundant, while the high peaks

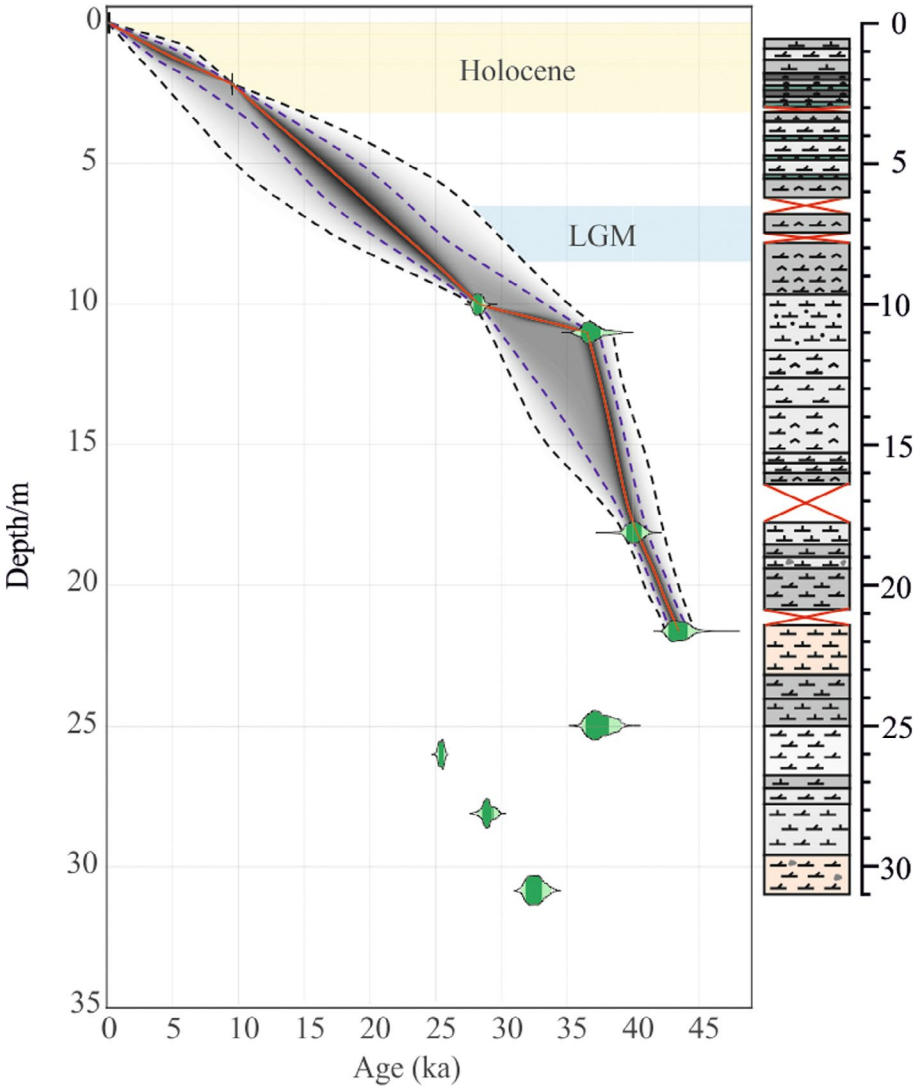

FIGURE 3 Depth-age model of Salinas Lake based on AMS ^{14}C ages. The black lines represent all iterations, while the red line indicates the most probable fit. The boundary between the Holocene and Pleistocene is located at approximately 3.5 m, where a significant change in lithology occurs, and laminated aragonite appears (Unit 4a). The last glacial maximum probably corresponds to the depth range of 7–9 m (Unit 5), characterised by dry, compact dolomite mud sediment.

TABLE 1 ^{14}C age and calibrated age based on IntCal20. 'Salinas-' were obtained by this study and used for age model reconstruction, while 'SAL-' were obtained by Giralt et al. (1999) from the same drilling site of Salines Lake, which can serve as a comparable age data set for this study.

Sample ID	Depth/m	14C age (years BP)	Calibrated median age
Salinas-1	2.17	8570 ± 50	9537
Salinas-2	10.02	24,040 ± 310	28,237
Salinas-3	11.02	32,300 ± 600	36,754
Salinas-4	18.13	34,900 ± 600	40,046
Salinas-5	21.64	40,000 ± 1100	43,420
Salinas-6	24.97	32,800 ± 600	37,418
Salinas-7	25.99	21,210 ± 170	25,534
Salinas-8	28.10	24,780 ± 350	29,018
Salinas-9	30.84	28,400 ± 440	32,604
SAL-1a	0.88	2830 ± 60	2943
SAL-1b	1.65	7400 ± 60	8229
SAL-1c	3.44	8810 ± 60	9854
SAL-1d	4.30	10,120 ± 60	11,710
SAL-1e	8.70	24,590 ± 250	28,828

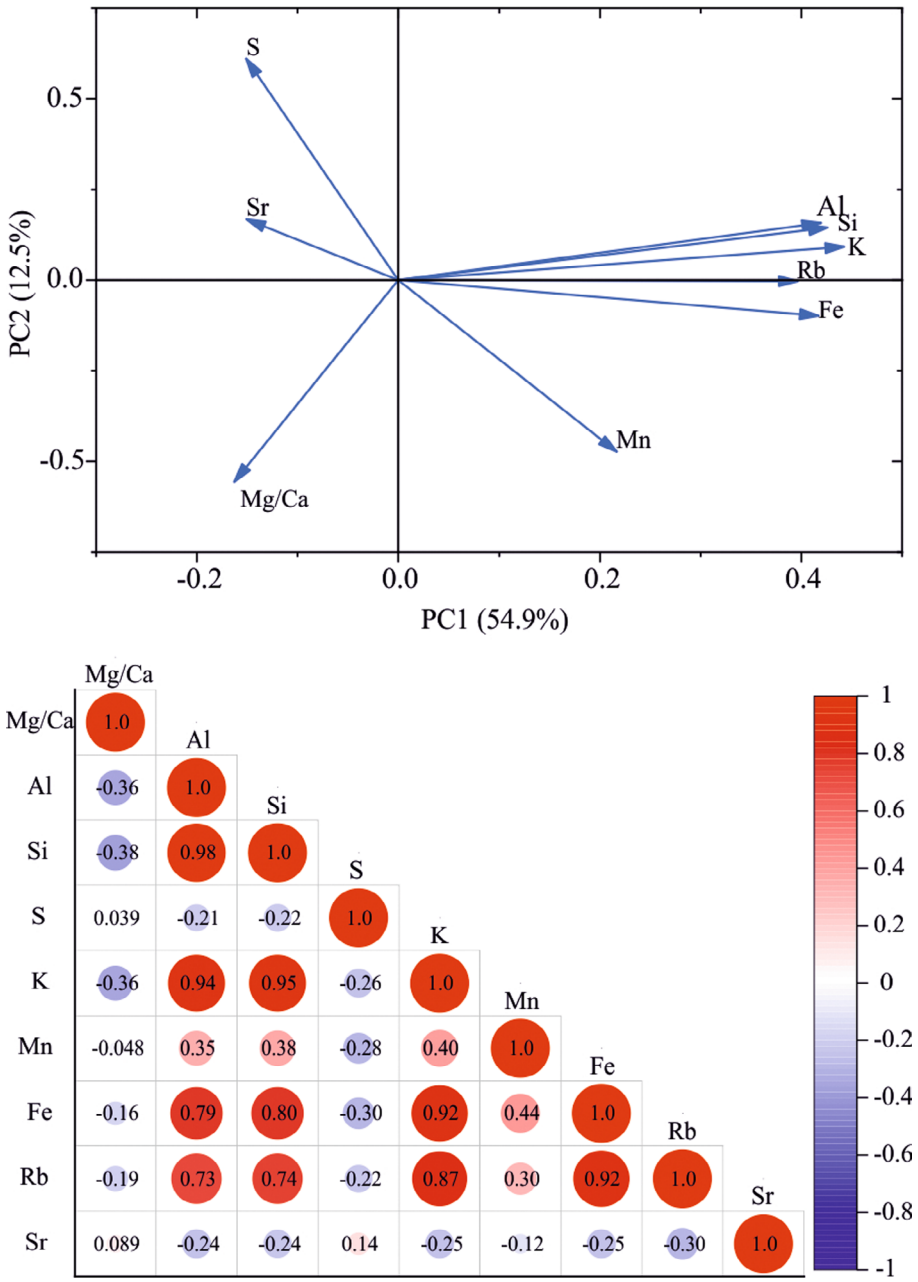

FIGURE 4 PCA and correlation analysis of XRF core scanning data. (A) Principal component analysis (PCA) of XRF core scanning data, highlighting the primary elemental associations. (B) Correlation matrix showing the relationships between elemental concentrations, providing insights into geochemical variations and depositional processes.

of siliciclastic elements coincide with calcite-rich sediment. This correlation possibly indicates dolomite depositing during arid phases.

4.4 | Stable oxygen and carbon isotopes

The $\delta^{13}C$ and $\delta^{18}O$ values exhibit big variance throughout the core, with $\delta^{13}C$ ranging from −6.5‰ to −2.4‰ (VPDB) and $\delta^{18}O$ from −2.3‰ to +4.9‰ (VPDB) (Figure 6). $\delta^{18}O$ values show a strong positive correlation with dolomite content ($R=0.72$, $p>0.05$) and are higher during dolomite-rich cycles.

A few samples were chosen for pore water extraction, and their $\delta^{13}C_{pw}$ and $\delta^{18}O_{pw}$ values were analysed (Table 2). The pore water $\delta^{13}C_{pw}$ values of dissolved inorganic carbon are significantly more positive (ranging from −0.59‰ to +11.97‰), while $\delta^{18}O_{pw}$ values are generally more negative than those of the dolomite samples, ranging from −30.99‰ to −29.17‰.

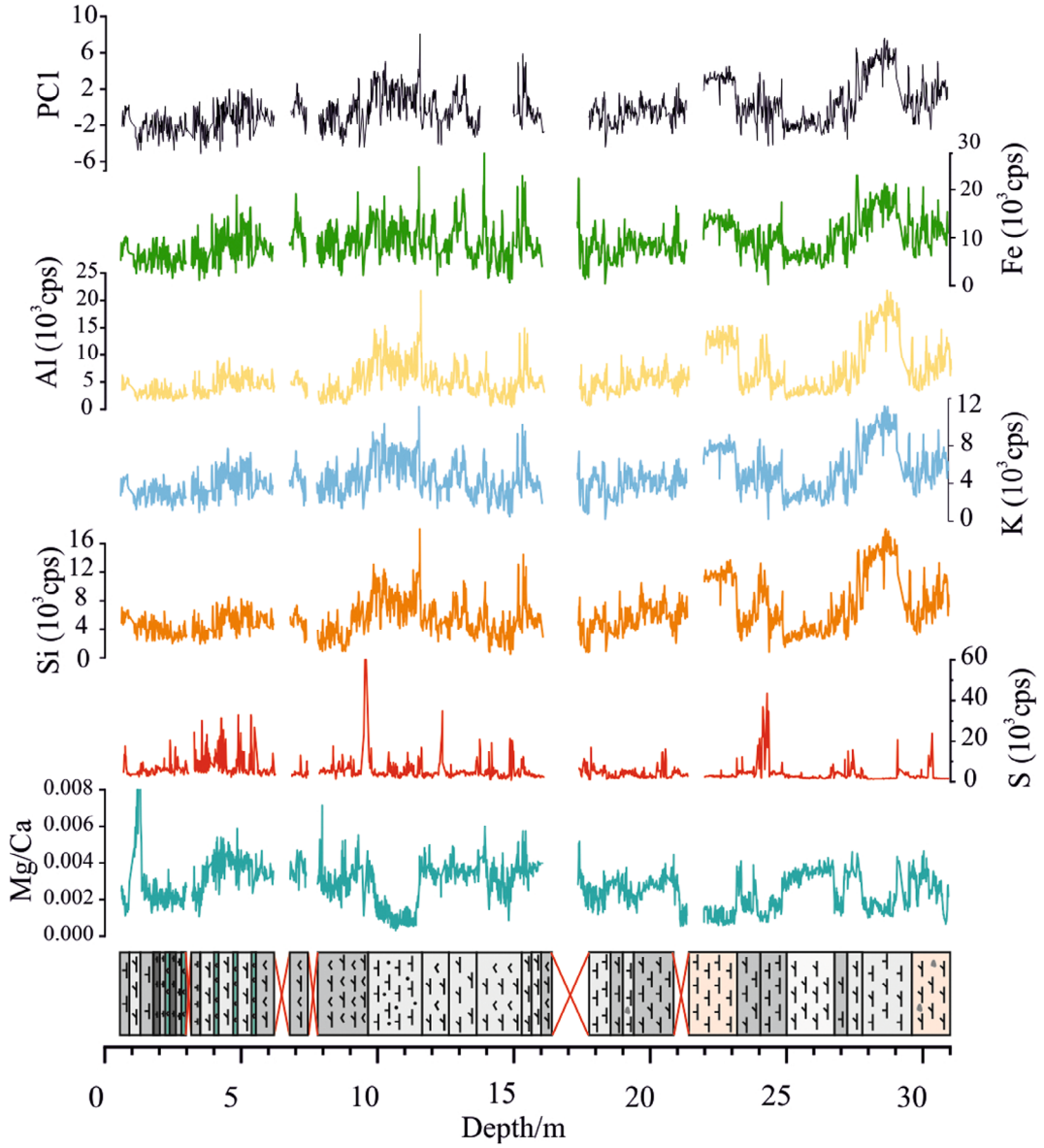

FIGURE 5 XRF core-scanning elemental concentrations (cps, counts per second). The Mg/Ca ratio reflects dolomite content, and S represents gypsum, as confirmed by XRD in Figure 3. The other elements are probably related to clastic input (e.g. quartz and clay minerals). Overall, the siliciclastic elements and PC1 in dolomite-rich sediment are much lower than the calcite-rich part, while S usually co-precipitates with dolomite. This correlation suggests dolomite tends to deposit in an arid phase.

4.5 | Characterisation of dolomite

Scanning electron microscopy (SEM) coupled with energy-dispersive X-ray spectroscopy (EDS) revealed the presence of rounded dolomite microcrystals (~1–1.5 μm in diameter) with central voids (Figure 7A,B) and spherical aggregates of dolomite crystals (Figure 7C,D). These microcrystals are closely associated with EPS, indicating a potential microbial influence on dolomite formation. Bacterial moulds were also observed (Figure 7B). As depth increases, the dolomite crystals show a transition to typical rhombohedral morphology (Figure 7E,F), suggesting a diagenetic evolution driven by increased burial and compaction over time.

4.6 | Organic geochemistry

The total organic carbon (TOC) content throughout the core is generally low, not exceeding 1.5% (Figure 6). Notable peaks in TOC occur at ~2.5, ~18 and ~27 m, all of which correspond to calcite-rich intervals. The average TOC values in dolomite-rich layers (0.27%) are lower than in calcite-rich layers (0.47%). The carbon-to-nitrogen

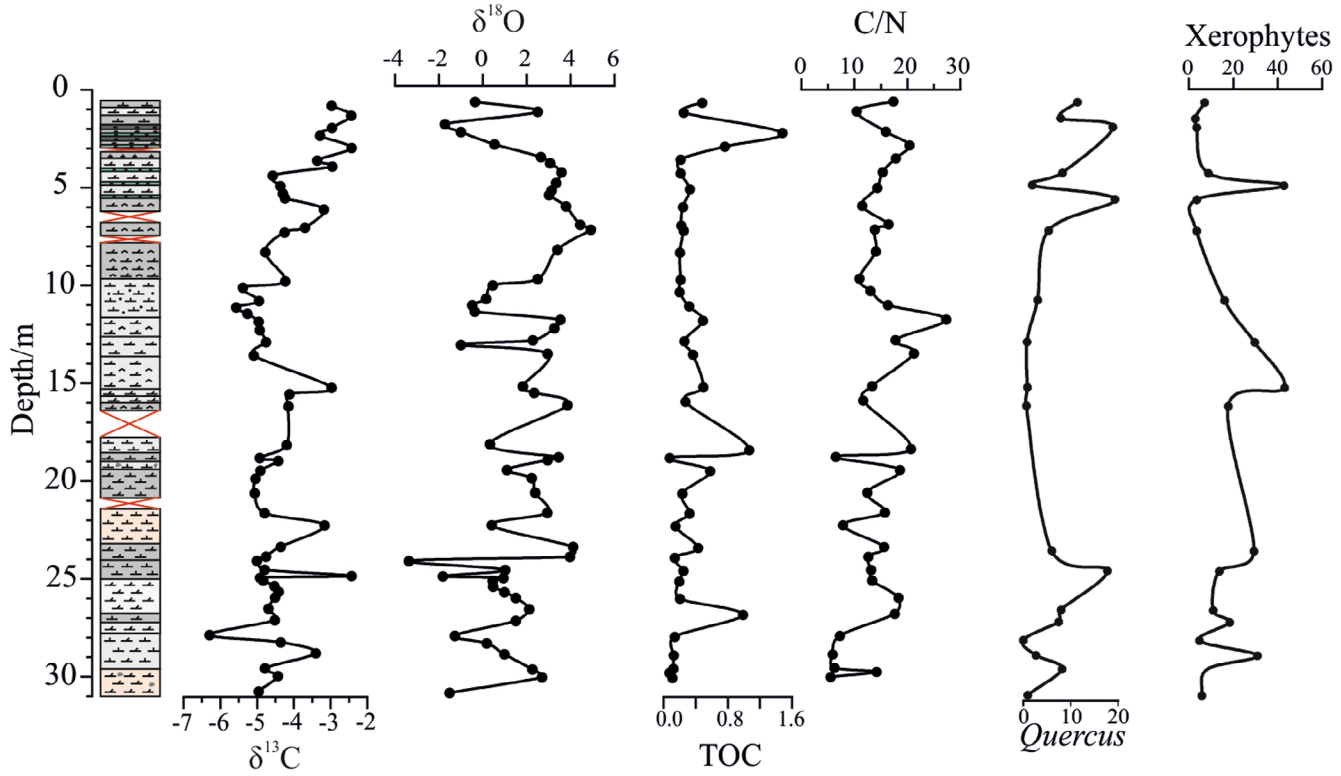

FIGURE 6 Plots of geochemical and pollen analysis results. From left to right: $\delta^{13}C$, $\delta^{18}O$, TOC and C/N ratio, followed by pollen results showing the percentages of Quercus and xerophytes.

TABLE 2 $\delta^{13}C$ and $\delta^{18}O$ of pore water (pw) and corresponding dolomites (dol).

Sample depth (m)	$\delta^{13}C_{pw}$ (VPDB, ‰)	$\delta^{18}O_{pw}$ (VPDB, ‰)	$\delta^{13}C_{dol}$ (VPDB, ‰)	$\delta^{18}O_{dol}$ (VPDB, ‰)
2.17	11.97	−30.80	−3.29	−0.99
2.81	8.59	−30.08	−2.43	0.53
5.16	3.82	−30.63	−4.30	3.13
9.69	−0.59	−30.96	−4.23	2.50
11.78	5.76	−31.00	−4.96	3.53
16.14	5.75	−30.41	−4.15	3.85
18.13	2.87	−29.57	−4.20	0.33
23.38	9.15	−29.18	−4.35	4.11
29.64	7.48	−30.65	−4.78	2.26

(C/N) ratios range from 5.4 to 27, with lower C/N values observed in the dolomite-rich sediments.

4.7 | Pollen sequence

A total of 19 palynological samples were collected throughout the core at different depths. The pollen data reveal that *Quercus* content remained low (never exceeding 20%) until the Holocene, when it increased. In contrast, xerophytic taxa were more abundant during the Pleistocene (up to 50%) and decreased dramatically during the Holocene, where their percentage dropped below 10%. This shift reflects the transition from the arid/cold Pleistocene to warm/humid conditions of the Holocene.

4.8 | Microbial community

Microbial community analysis was conducted on four sediment samples taken from different lithological units at various depths. The microbial communities were dominated by four families: *Halomonadaceae*, *Rhodobacteraceae*, *Thioalkalibacteraceae* and *Bacillaceae*, all of which include halophilic bacteria (Figure 8). Sediment samples S1 and

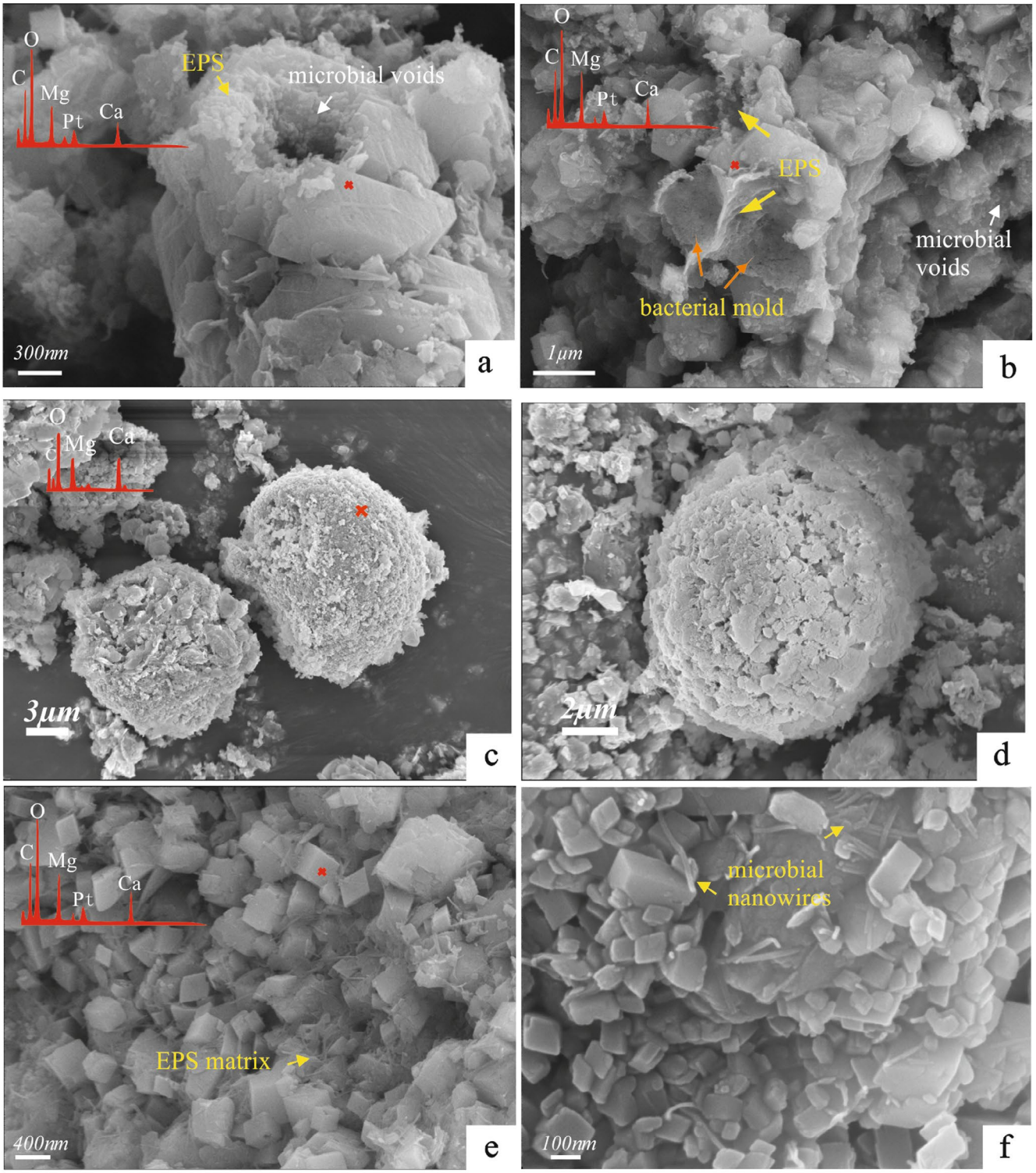

FIGURE 7 SEM images with EDS of dolomite samples from different depths of the core. (A, B) Top (~1 m), (C, D) middle (~18 m), (E, F) bottom (~25 m) of the core. EDS analysis confirms XRD data, displaying high peaks of Mg, Ca, O and C, with a Pt peak corresponding to the coating. Voids with diameters of approximately 1 μm (white arrows) are observed in the centre of rounded dolomite crystals (A, B), alongside bacterial moulds (orange arrows) attached to a dolomite crystal. Additionally, spheroidal dolomite crystal aggregation with a porous surface was observed (C, D). As depth increases, dolomite transitions from a rounded to a rhombohedral morphology (E, F). Despite this change, remnants of the EPS matrix and microbial nanowires, where nanocrystals of dolomite nucleate, remain well preserved. The different dolomite morphologies at the top and bottom of the core illustrate the ageing process of dolomite during lithification, occurring with increasing burial depth and time. This emphasises the importance of Salinas Lake for studying the 'dolomite problem'.

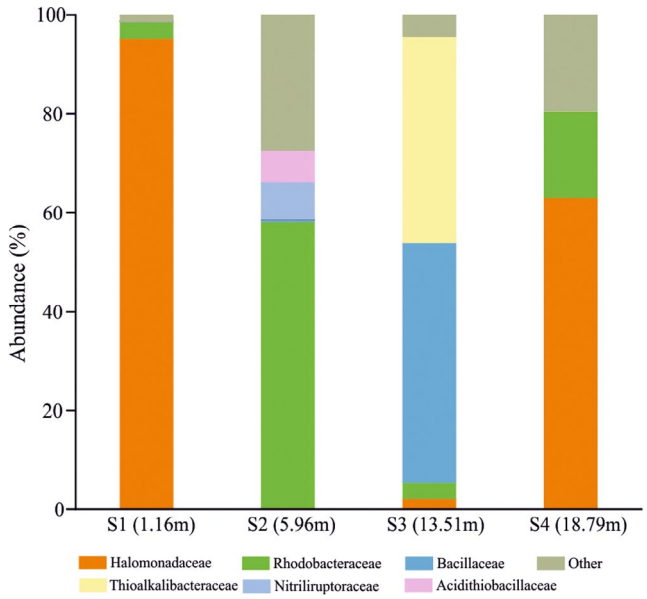

FIGURE 8 Abundance of microbial communities in Salinas sediments at different depths. The dominant microbial families in samples S1 and S4 are *Halomonadaceae*, the largest family of halophiles. In contrast, for samples S2 and S3, the dominant families are *Rhodobacteraceae*, *Thioalkalibacteraceae* and *Bacillaceae*, which are halotolerant bacteria commonly found in saline lakes. The predominance of halophilic microbes in the Salinas sediments indicates a saline environment.

S4 were primarily dominated by *Halomonadaceae*, while *Rhodobacteraceae*, *Thioalkalibacteraceae* and *Bacillaceae* were more abundant in S2 and S3.

Halomonadaceae is the largest family composed of halophilic bacteria, containing either slight or moderate halophiles or halotolerant (De la Haba et al., 2023). *Thioalkalibacteraceae* are obligate halophiles, requiring at least 0.4 M NaCl (Boden, 2017). Many species of *Rhodobacteraceae* and *Bacilliaceae* require NaCl for growth (Boone et al., 2005; Vos et al., 2011). The presence of halophilic bacteria supports the saline environment observed in other sections of the study.

5 | DISCUSSION

5.1 | Properties and origin of Salinas dolomite

Dolomite is a key mineral in lacustrine sedimentary environments and is widely recognised for its utility in palaeoclimate reconstruction (Guo, Wen, Li, et al., 2023; Guo, Wen, & Sánchez-Román, 2023; McCormack et al., 2019; Sánchez-Román et al., 2023, 2025; Sánchez-Román, McKenzie, et al., 2011; Sánchez-Román, Romanek, et al., 2011; Talbot, 1990; Yao et al., 2024). For example, its oxygen isotope composition, which is sensitive to environmental parameters such as temperature, humidity, salinity and the isotopic composition of lake water, can provide valuable insights into past climate and environmental conditions (Liutkus & Wright, 2008; Horton et al., 2016; Hudson et al., 2017; McCormack & Kwiecien, 2021; Sánchez-Román et al., 2009, 2023).

In the context of Salinas Lake, the primary source of dolomite is potentially a combination of detrital inputs from surrounding Mesozoic dolostones, which occur alongside siliciclastic minerals, and authigenic formation possibly facilitated by microbial activity, which plays an integral role in mineral precipitation under hypersaline and evaporitic conditions (Aldisi et al., 2017; Alibrahim et al., 2019; Bontognali et al., 2010; Qiu et al., 2017; Sánchez-Román et al., 2007, 2009, 2023; Wen et al., 2020; Zhao et al., 2023). The distinction between detrital and authigenic dolomite is crucial for palaeoclimatic reconstructions, as detrital dolomite reflects only the characteristics of the source rock, whereas authigenic dolomite records *in situ* environmental conditions and provides a more direct palaeoclimate signal.

Firstly, geochemical evidence suggests that Salinas dolomite is dominantly of authigenic origin. Both XRD and XRF data reveal that quartz and siliciclastic elements (e.g. Si) are enriched in calcite-dominated sediments, whereas dolomite-dominated intervals coincide with elevated gypsum and sulphur contents, typical of evaporative settings (Figures 2 and 5). Moreover, a negative correlation between Mg/Ca ratios and siliciclastic elements (Figure 4) further excludes significant detrital contributions.

Microscopic observations provide additional support. SEM imaging reveals euhedral nanocrystals embedded within EPS (Figure 7B,E), consistent with microbially mediated precipitation (Bontognali et al., 2008; Sánchez-Román et al., 2008, 2023; Yao et al., 2024). The presence of bacterial voids within the dolomite crystals and bacterial moulds provides additional evidence for microbial involvement, as such features are typical characteristics of bacterially mediated carbonate precipitation (Sánchez-Román et al., 2014, 2023, 2025; Yao et al., 2024). Moreover, the observed transition from spherical to angular, rhombohedral morphologies with increasing depth (Figure 7) is consistent with dolomite ageing processes (Petrash et al., 2017).

Microbial community and stable isotope data further reinforce the microbial origin of Salinas dolomite. In Salinas Lake, the microbial assemblages are dominated by obligate halophilic or halotolerant bacteria, primarily including *Halomonadaceae*, *Thioalkalibacteraceae*, *Rhodobacteraceae* and *Bacillaceae*. Dolomite precipitation mediated by these halophilic microbes has not only been documented in modern lacustrine environments, such as

the Coorong Lakes in South Australia (Wacey et al., 2007), Brejo do Espinho Lagoon (Sánchez-Román et al., 2009a) andLagoa Vermelha (Vasconcelos & Mckenzie, 1997) in Brazil but also reported in controlled laboratory culture experiments (Aldisi et al., 2017; Alibrahim et al., 2019; Helmi et al., 2016; Sánchez-Román et al., 2008, 2009). The negative $\delta^{13}C$ values (Figure 6) additionally support microbial mediation, as microbial processes involving organic matter typically lead to depleted $\delta^{13}C$ signatures (Braissant et al., 2007; Sánchez-Román et al., 2009, 2025; Sánchez-Román, McKenzie, et al., 2011; Vasconcelos & McKenzie, 1997). Moreover, the relatively positive $\delta^{13}C$ of dissolved inorganic carbon (DIC) in pore water (Table 2) suggests that inorganic carbon is not the carbon source for dolomite formation. Besides, comparisons with other modern saline lakes show that the $\delta^{18}O$ values in Salinas Lake (−2.3 to +4.9‰) fall within the range reported for highly evaporative systems (Figure 9), which provide favourable conditions for the proliferation of halophilic bacteria.

Collectively, these lines of evidence strongly support a microbial, authigenic origin for dolomite in Salinas Lake.

5.2 | Carbonate mineral cycles and climate control

Modern environments where dolomite precipitates, such as hypersaline lagoons and evaporative lakes, serve as valuable analogues for understanding the mechanisms driving dolomite formation (Sánchez-Román et al., 2009; Vasconcelos & McKenzie, 1997; Areias et al., 2022; Naim et al., 2025). The dynamic hydrological conditions of Salinas Lake, combined with fluctuating carbonate concentrations, make it an ideal system for studying the interactions between local climate variations and mineral precipitation.

Compared to the calcite-rich sediments, the dolomitic intervals in Salinas Lake display more positive $\delta^{18}O$ values, lower total organic carbon (TOC) and C/N ratios and reduced concentrations of siliciclastic elements (Al, Si, K, Fe). The low TOC values usually suggest a shallow, non-stratified, closed lake environment with an oxygenated bottom (Qiu et al., 2021). C/N ratios below 10 are typical of algal-derived organic matter and generally indicate an autochthonous lacustrine source, whereas higher values reflect greater contributions from terrestrial plants (Meyers & Lallier-Vergès, 1999; Morellon et al., 2009). Therefore, the lower TOC and C/N ratios, combined with the reduced abundance of siliciclastic elements, suggest diminished clastic input (i.e. more arid climate) during dolomite precipitation. The $\delta^{18}O$ data further supports this interpretation, indicating more intense evaporation during dolomite formation. In lacustrine environments, the $\delta^{18}O$ of carbonates is influenced by both temperature and the isotopic composition of lake water (Guo, Wen, Li, et al., 2023; Liutkus & Wright, 2008; McCormack & Kwiecien, 2021; Rosen et al., 1995; Sánchez-Román et al., 2009, 2023; Yao et al., 2024). Based on the $\delta^{18}O$

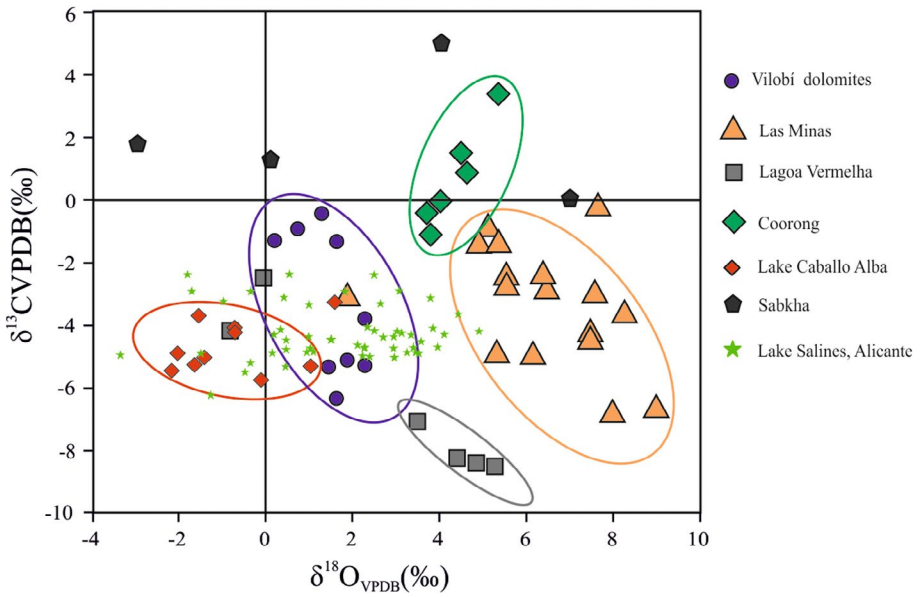

FIGURE 9 Cross-plot of measured $\delta^{13}C$ and $\delta^{18}O$ values of dolomites from various modern and ancient environments. This plot includes dolomite samples from modern environments such as Salinas (this study), Sabkha (Bontognali et al., 2010), Lake Caballo Alba (Sánchez-Román et al., 2023), Brejo do Espinho (Sánchez-Román et al., 2009) and Lagoa Vermelha (Vasconcelos & McKenzie, 1997). Additionally, ancient dolomites from Las Minas (Pineda et al., 2021) and Vilobí (Sánchez-Román et al., 2023) are also presented for comparison.

fractionation equation for dolomite–water proposed by Vasconcelos et al., (2005), a 1°C increase in temperature would result in an enrichment of approximately +0.24‰ in the $\delta^{18}O$ value of dolomite. However, the isotopic composition of lake water is also controlled by the balance between meteoric inputs and evaporative losses. Evaporation preferentially removes isotopically lighter oxygen, enriching the residual water in heavier isotopes (Ma et al., 2017; Wang et al., 2020). This process has been confirmed experimentally, with laboratory studies demonstrating a positive correlation between salinity and $\delta^{18}O$ values (Lloyd, 1966). Given the wide range of $\delta^{18}O$ values observed in Salinas dolomite (−2.3‰ to +4.9‰), evaporation rather than temperature appears to be the dominant control, reflecting highly evaporative conditions during dolomite precipitation. The scarcity of quartz, typically associated with enhanced run-off, further supports reduced detrital input during dolomitic intervals. Moreover, the association of dolomite with gypsum and sulphur peaks strongly suggests precipitation in an evaporative environment.

The chronology results indicate that the Salinas core spans from the late Pleistocene, which is characterised by short and abrupt global climatic oscillations between interstadial and stadial in centennial to millennial scales, known as 'Dansgaard–Oeschger cycles' (D-O cycles) (Bolton et al., 2010; Dansgaard et al., 1993; Fletcher et al., 2010), and at least 25 D-O cycles were identified based on $\delta^{18}O$ of NGRIP (North Greenland Ice Core) (Held et al., 2024; NGRIP members, 2004; Schannwell et al., 2024). The alternation of mineralogy between calcite and dolomite in Salinas Lake sediment is highly potentially a result of lake hydrological responses to rapid climatic changes. The LGM (last glacial maximum), a globally cooler and drier interval characterised by lower temperature, descending sea level, proliferation of steppe and contraction of forests in most European regions (Cascalheira et al., 2021; Chondrogianni et al., 2004; Valero-Garcés et al., 2004), was also identified in Salinas Lake sediment, corresponding to Unit 5 that is characterised by dry and compact dolomite mud sediment with enrichment of gypsum and high $\delta^{18}O$ values, features of enhanced evaporation and high salinity, indicating arid climate. Palynological data showing almost an absence of *Quercus* and a much higher percentage of xerophytes (Figure 6) further confirm the arid conditions.

A significant shift occurs near 3.5 m depth (Unit 4a, approximately corresponding to 11–7 cal ka BP), marking the onset of the Holocene. Here, mineralogy transits from dolomite–gypsum dominance to calcite-rich deposits with aragonite. This change, alongside more negative $\delta^{18}O$ values, elevated quartz content and higher TOC and C/N ratios, represents higher lake productivity and run-off input. This humid phase aligns with the warmer and moister climate of the Holocene compared to the preceding Pleistocene, a period characterised by the expansion of deciduous forests across Mediterranean regions (Camuera et al., 2019; Fletcher & Goñi, 2008; Magny et al., 2002; Marcott et al., 2013), a pattern also recorded in the Salinas Lake sedimentary sequence (Figure 6).

In summary, Salinas Lake records alternations between arid (dolomite-dominated) and humid (calcite-dominated) phases, tightly controlled by climate-driven hydrological changes.

5.3 | The role of microbial activities in dolomite precipitation

In modern oceans, although the sea water is supersaturated with respect to dolomite, the strong hydration shell of Mg^{2+} ions hinders direct precipitation of dolomite from the sea water column (Lippmann, 1973). Remarkably, a long-term laboratory experiment attempting to precipitate dolomite under ambient conditions also failed (Land, 1998). Therefore, mechanisms beyond climate control are necessary to facilitate dolomite precipitation.

In hypersaline environments such as coastal sabkhas (e.g. Abu Dhabi, Dohat Faishakh), dolomite precipitation within microbial mats has been well documented (Bontognali et al., 2010; Brauchli et al., 2016; DiLoreto et al., 2019). Laboratory culture experiments using microbes isolated from these hypersaline microbial mats, especially halophilic bacteria and cyanobacteria, have successfully precipitated high-Mg calcite and proto-dolomite under the Earth surface conditions (Aldisi et al., 2017; Alibrahim et al., 2019; Deng et al., 2010; Popall et al., 2020; Sánchez-Román et al., 2011b, 2025). Consequently, microbial activity and the presence of microbial mats have been proposed as key factors in dolomite precipitation. The hypersaline and evaporative conditions can induce ecological stress in microbial communities, stimulating the production of large amounts of EPS, which constitute most of the microbial mats to prevent the microbes from the harsh environment (Sánchez-Román et al., 2023). These microbial mats play a crucial role in dolomite precipitation by sustaining high pH and alkalinity, as well as absorbing Mg ions into carbonates and providing nucleation sites for following crystal growth (Bontognali et al., 2010; Brauchli et al., 2016; Petrash et al., 2015; Popall et al., 2020; Sánchez-Román et al., 2009, 2023; del Buey et al., 2023).

Similar to these hypersaline environments, the prevalence of EPS in Salinas sediment, along with the

hollow centres observed in dolomite crystals under SEM (Figure 7), strongly points to microbial mediation. Besides, microbial community analysis reveals a dominance by obligate halophilic or halotolerant bacteria, mainly including *Halomonadaceae*, *Thioalkalibacteraceae*, *Rhodobacteraceae* and *Bacillaceae*. Notably, several genera such as *Halomonas*, *Virgibacillus* and *Bacillus*, members of the families *Halomonadaceae* and *Bacillaceae*, have been shown to successfully catalyse the precipitation of carbonates in multiple culture experiments (Aldisi et al., 2017; Alibrahim et al., 2019; Helmi et al., 2016; Sánchez-Román et al., 2007; Sánchez-Román, Romanek, et al., 2011). Therefore, both sedimentological observations and microbiological data strongly support microbial mediation in the dolomite precipitation process in Salinas Lake.

5.4 | Integrated model: climate, microbial activity and carbonate precipitation

Our findings suggest a dynamic interplay between regional climate, microbial activity and carbonate mineral formation in Salinas Lake (Figure 10). During arid periods characterised by high evaporation-to-precipitation (E/P) ratios, lake waters became increasingly saline, leading to elevated concentrations of Ca^{2+} and Mg^{2+} ions and promoting dolomite saturation (Popall et al., 2020; Sánchez-Román et al., 2009, 2023). These hypersaline conditions also favoured the proliferation of microbial mats, which enhanced dolomite precipitation through the production of EPS and biological mediation (Bontognali et al., 2010; Braissant et al., 2007; Popall et al., 2020; Figure 10B). Conversely, during more humid climatic phases, dilution of hypersaline lake waters lowered salinity and reduced the habitability for obligate halophilic microorganisms, leading to decreased dolomite saturation and a decline in microbial mat development. Under such conditions, carbonate precipitation favoured minerals such as calcite and aragonite (Figure 10A).

The integrated effect of evaporation-driven salinity changes, microbial mediation and regional climate variability provides a comprehensive framework for understanding the processes governing dolomite formation in Salinas Lake. This model aligns with observations from other lacustrine and sabkha environments where climate-driven hydrology controls mineral precipitation dynamics mediated by microbial communities (Guo, Wen, Li, et al., 2023; Guo, Wen, & Sánchez-Román, 2023; Sánchez-Román et al., 2023).

6 | CONCLUSION

Salinas Lake, a hypersaline playa lake in southern Iberia, serves as a modern analogue for dolomite precipitation in saline lacustrine environments. The combined geochemical signatures ($\delta^{13}C$ and $\delta^{18}O$), SEM-observed dolomite morphologies and associated microbial features, such as filamentous structures and empty spheroidal

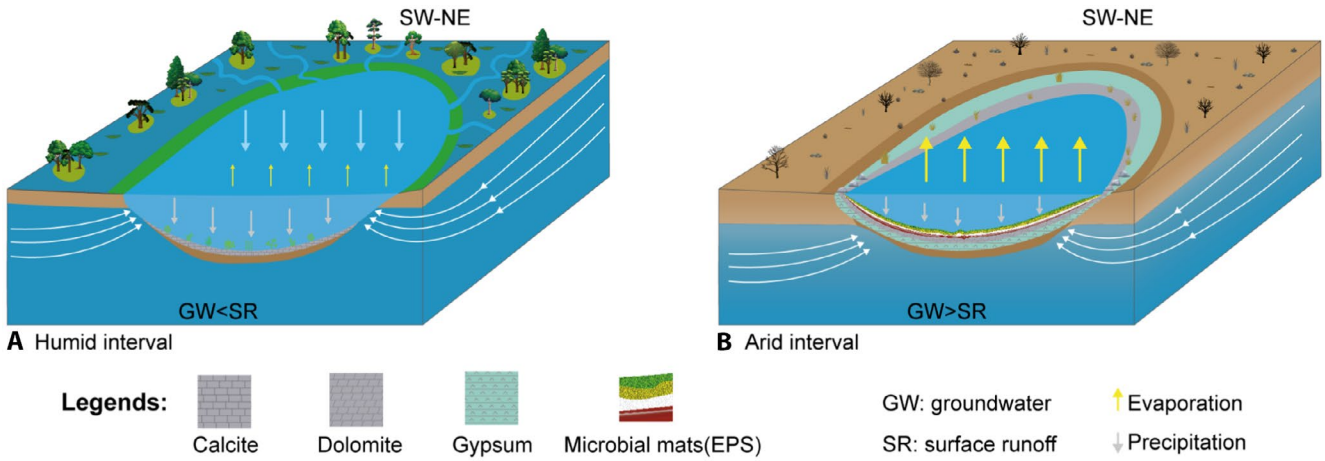

FIGURE 10 Schematic graph of climate and environmental influence on lake geochemistry and dolomite precipitation. During arid phases, such as the LGM, when precipitation is lower than evaporation, the concentrations of Mg^{2+} and Ca^{2+} ions increase, promoting dolomite saturation. During these periods, the lake was primarily replenished by saline groundwater rather than fresh run-off, leading to a highly saline waterbody conducive to the formation of microbial mats. These mats absorb metal ions (such as Ca, Mg and Fe) and catalyse dolomite precipitation, resulting in the deposition of dolomite and co-precipitation of gypsum. In contrast, during relatively humid phases (e.g. the Holocene), when the water balance is positive, the lake receives fresher run-off. This not only dissolved Ca^{2+} from the surrounding Tertiary limestone mountains but also diluted the lake water, fostering conditions favourable for the precipitation of calcite and aragonite. The cyclical nature of arid and humid phases led to the alternating deposition of dolomite-rich and calcite-rich sediments.

microcrystalline aggregates, strongly support a microbial role in dolomite formation under the lake's saline conditions.

This study explored how late Pleistocene and Holocene climatic and hydrological fluctuations influenced dolomite precipitation at Salinas Lake. By integrating geochemical, pollen and stable isotope data, we documented alternating arid and humid phases characterised by rapid stadial-interstadial oscillations, probably driven by Dansgaard–Oeschger cycles. These climatic shifts controlled sediment lithology and geochemical proxies, reflecting the terrestrial response to global palaeoclimate events. The Holocene transition to warmer, wetter conditions led to the establishment of a permanent lake and the precipitation of aragonite. Mineral assemblages, particularly the occurrence of dolomite-rich layers, closely track these climate-driven environmental changes, highlighting a tight coupling between regional palaeoclimate and lacustrine dolomite formation. Beyond climatic control, microbial mediation was also crucial, especially during arid phases where hypersalinity and evaporative conditions promoted secretion of EPS by halophilic microorganisms, facilitating dolomite precipitation.

By integrating mineralogical, geochemical and microbial evidence, this work advances understanding of the complex interactions among climate, hydrology, microbial activity and dolomite formation in lacustrine settings. Furthermore, it demonstrates the potential of low-temperature dolomite as a proxy for reconstructing past climate and hydrological conditions, with implications for analogous environments worldwide.

ACKNOWLEDGEMENTS

This work was supported by the Dutch Research Council (NWO) Projects: OCENW.KLEIN.037 and ENW.GO.001.033 to MSR. GL acknowledges PhD CSC scholarship Nr. 202106370036. MSR also acknowledges support from Beatriz Galindo Senior Fellowship (No. BG23-00132) funded by the Spanish Ministry of Science, Innovation and Universities (MICIU). We gratefully acknowledge Susan Verdegaal and Martina Haagen for their assistance with stable isotope and organic matter analyses, respectively. We also thank Willem-Jan Blom for his support in defining the age model. Our appreciation extends to Piet van Gaever at NIOZ for his help with XRF analyses. Javier Jaimez Águila (CIC-UGR, Granada, Spainm), L. Gibert Leria and A. Vicente Gibert and Jose Sanchez Herrero are deeply acknowledged for their essential assistance during the drilling a,operations. The Salinas Town Hall (Alicante, Spain) is gratefully ackowldged for facilitating the drilling permits. Finally, we thank the editor-in-chief, associate editor, and two anonymous reviewers for their time and constructive feedback, which helped to improve the quality of this manuscript.

CONFLICT OF INTEREST STATEMENT

We declare that no conflict of interest is to be disclosed.

DATA AVAILABILITY STATEMENT

The data underlying this article are available in the Mendeley Data repository (https://data.mendeley.com), at https://doi.org/10.17632/8ymv436w2r.1.

ORCID

Zeina Naim https://orcid.org/0009-0001-2868-4884

REFERENCES

Aldisi, Z.A., Jaoua, S., Bontognali, T.R.R., Attia, E.S.M., Al-Kuwari, H.A.A.S. & Zouari, N. (2017) Evidence of a Role for Aerobic Bacteria in High Magnesium Carbonate Formation in the Evaporitic Environment of Dohat Faishakh Sabkha in Qatar. *Frontiers in Environmental Science*, 5, 1. https://doi.org/10.3389/fenvs.2017.00001

Alibrahim, A., Al-Gharabally, D., Mahmoud, H. & Dittrich, M. (2019) Proto-dolomite formation in microbial consortia dominated by Halomonas strains. *Extremophiles*, 23, 765–781.

Areias, C., Barbosa, C.F., Cruz, A.P.S., McKenzie, J.A., Ariztegui, D., Eglinton, T., Haghipour, N., Vasconcelos, C. & Sánchez-Román, M. (2022) Organic Matter Diagenesis and precipitation of MG-Rich Carbonate and Dolomite in Modern Hypersaline Lagoons linked to climate changes. *Geochimica et Cosmochimica Acta*, 337, 14–32. https://doi.org/10.1016/j.gca.2022.09.030

Battarbee, R.W. (2000) Palaeolimnological approaches to climate change, with special regard to the biological record. *Quaternary Science Reviews*, 19, 107–124.

Beug, H.-J. (2004) *Leitfaden der Pollenbestimmung für Mitteleuropa und angrenzende Gebiete*. (No Title).

Boden, R. (2017) Reclassification of *Halothiobacillus hydrothermalis* and *Halothiobacillus halophilus* to Guyparkeria gen. nov. in the Thioalkalibacteraceae fam. nov., with emended descriptions of the genus Halothiobacillus and family Halothiobacillaceae. *International Journal of Systematic and Evolutionary Microbiology*, 67, 3919–3928.

Bokulich, N.A., Kaehler, B.D., Rideout, J.R., Dillon, M., Bolyen, E., Knight, R., Huttley, G.A. & Gregory Caporaso, J. (2018) Optimizing taxonomic classification of marker-gene amplicon sequences with QIIME 2's q2-feature-classifier plugin. *Microbiome*, 6, 1–17.

Bolton, C.T., Wilson, P.A., Bailey, I., Friedrich, O., Beer, C.J., Becker, J., Baranwal, S. & Schiebel, R. (2010) Millennial-scale climate variability in the subpolar North Atlantic Ocean during the late Pliocene. *Paleoceanography*, 25(4).

Bolyen, E., Rideout, J.R., Dillon, M.R., Bokulich, N.A., Abnet, C.C., Al-Ghalith, G.A., Alexander, H., Alm, E.J., Arumugam, M. & Asnicar, F. (2019) Reproducible, interactive, scalable and extensible microbiome data science using QIIME 2. *Nature Biotechnology*, 37, 852–857.

Bontognali, T.R., Vasconcelos, C., Warthmann, R.J., Bernasconi, S.M., Dupraz, C., Strohmenger, C.J. & McKenzie, J.A. (2010) Dolomite formation within microbial mats in the coastal sabkha of Abu Dhabi (United Arab Emirates). *Sedimentology*, 57, 824–844.

Bontognali, T.R., Vasconcelos, C., Warthmann, R.J., Dupraz, C., Bernasconi, S.M. & McKenzie, J.A. (2008) Microbes produce nanobacteria-like structures, avoiding cell entombment. *Geology*, 36, 663–666.

Boone, D., Goodfellow, M., Rainey, F., Schleifer, K. & Vos, P. (2005) *Bergey's manual of systematic bacteriology: volume 2: the Proteobacteria Part C The Alpha-, Beta-, Delta-, and Epsilonproteobacteria*. New York: Springer.

Braissant, O., Decho, A.W., Dupraz, C., Glunk, C., Przekop, K.M. & Visscher, P.T. (2007) Exopolymeric substances of sulfate-reducing bacteria: interactions with calcium at alkaline pH and implication for formation of carbonate minerals. *Geobiology*, 5, 401–411.

Brauchli, M., McKenzie, J.A., Strohmenger, C.J., Sadooni, F., Vasconcelos, C. & Bontognali, T.R. (2016) The importance of microbial mats for dolomite formation in the Dohat Faishakh sabkha, Qatar. *Carbonates and Evaporites*, 31, 339–345.

Burjachs, F., Jones, S.E., Giralt, S. & De Pablo, J.F.-L. (2016) Lateglacial to Early Holocene recursive aridity events in the SE Mediterranean Iberian Peninsula: the Salines playa lake case study. *Quaternary International*, 403, 187–200.

Camuera, J., Jiménez-Moreno, G., Ramos-Román, M.J., García-Alix, A., Toney, J.L., Anderson, R.S., Jiménez-Espejo, F., Bright, J., Webster, C. & Yanes, Y. (2019) Vegetation and climate changes during the last two glacial-interglacial cycles in the western Mediterranean: a new long pollen record from Padul (southern Iberian Peninsula). *Quaternary Science Reviews*, 205, 86–105.

Cascalheira, J., Alcaraz-Castano, M., Alcolea-Gonzalez, J., De Andrés-Herrero, M., Arrizabalaga, A., Tortosa, J.E.A., Garcia-Ibaibarriaga, N. & Iriarte-Chiapusso, M.-J. (2021) Paleoenvironments and human adaptations during the Last Glacial Maximum in the Iberian Peninsula: a review. *Quaternary International*, 581, 28–51.

Chen, T., Qiu, X., Liu, D., Papineau, D., Wang, H., Dai, Z., Bontognali, T.R. & Benzerara, K. (2024) Dissolved silicon as a beneficial factor for biomineralization of disordered dolomite by a halophilic cyanobacterium. *Chemical Geology*, 670, 122435.

Chondrogianni, C., Ariztegui, D., Rolph, T., Juggins, S., Shemesh, A., Rietti-Shati, M., Niessen, F., Guilizzoni, P., Lami, A. & McKenzie, J.A. (2004) Millennial to interannual climate variability in the Mediterranean during the Last Glacial Maximum. *Quaternary International*, 122, 31–41.

Dansgaard, W., Johnsen, S.J., Clausen, H.B., Dahl-Jensen, D., Gundestrup, N.S., Hammer, C.U., Hvidberg, C.S., Steffensen, J.P., Sveinbjörnsdottir, A. & Jouzel, J. (1993) Evidence for general instability of past climate from a 250-kyr ice-core record. *Nature*, 364, 218–220.

Daye, M., Higgins, J. & Bosak, T. (2019) Formation of ordered dolomite in anaerobic photosynthetic biofilms. *Geology*, 47, 509–512.

De La Haba, R.R., Arahal, D.R., Sánchez-Porro, C., Chuvochina, M., Wittouck, S., Hugenholtz, P. & Ventosa, A. (2023) A long-awaited taxogenomic investigation of the family Halomonadaceae. *Frontiers in Microbiology*, 14, 1293707.

del Buey, P., Sanz-Montero, M.E. & Sánchez-Román, M. (2023) Bioinduced precipitation of smectites and carbonates in photosynthetic diatom-rich microbial mats: effect of culture medium. *Applied Clay Science*, 238, 106932. https://doi.org/10.1016/j.clay.2023.106932

Deng, S., Dong, H., Lv, G., Jiang, H., Yu, B. & Bishop, M.E. (2010) Microbial dolomite precipitation using sulfate reducing and halophilic bacteria: results from Qinghai Lake, Tibetan Plateau, NW China. *Chemical Geology*, 278, 151–159.

DiLoreto, Z.A., Bontognali, T.R., Al Disi, Z.A., Al-Kuwari, H.A.S., Williford, K.H., Strohmenger, C.J., Sadooni, F., Palermo, C., Rivers, J.M. & McKenzie, J.A. (2019) Microbial community composition and dolomite formation in the hypersaline microbial mats of the Khor Al-Adaid sabkhas, Qatar. *Extremophiles*, 23, 201–218.

Faegri, K., Iversen, J., Kaland, P.E. & Krzywinski, K. (1989) *Textbook of pollen analysis*. Caldwell, NJ: Blackburn Press.

Fang, Y., Hobbs, F., Yang, Y. & Xu, H. (2023) Dissolved silica-driven dolomite precipitation in the Great Salt Lake, Utah, and its implication for dolomite formation environments. *Sedimentology*, 70, 1328–1347.

Fletcher, W.J. & Goñi, M.F.S. (2008) Orbital-and sub-orbital-scale climate impacts on vegetation of the western Mediterranean basin over the last 48,000 yr. *Quaternary Research*, 70, 451–464.

Fletcher, W.J., Goni, M.F.S., Allen, J.R., Cheddadi, R., Combourieu-Nebout, N., Huntley, B., Lawson, I., Londeix, L., Magri, D. & Margari, V. (2010) Millennial-scale variability during the last glacial in vegetation records from Europe. *Quaternary Science Reviews*, 29, 2839–2864.

García-Alix, A., Jiménez-Moreno, G., Gázquez, F., Monedero-Contreras, R., López-Avilés, A., Jiménez-Espejo, F.J., Rodríguez-Rodríguez, M., Camuera, J., Ramos-Román, M.J. & Anderson, R.S. (2022) Climatic control on the Holocene hydrology of a playa-lake system in the western Mediterranean. *Catena*, 214, 106292.

Geske, A., Lokier, S., Dietzel, M., Richter, D., Buhl, D. & Immenhauser, A. (2015) Magnesium isotope composition of sabkha porewater and related (Sub-) Recent stoichiometric dolomites, Abu Dhabi (UAE). *Chemical Geology*, 393, 112–124.

Giralt, S., Burjachs, F., Roca, J. & Julià, R. (1999) Late Glacial to Early Holocene environmental adjustment in the Mediterranean semi-arid zone of the Salinas playa-lake (Alacant, Spain). *Journal of Paleolimnology*, 21, 449–460.

Giralt, S., Moreno, A., Bao, R., Sáez, A., Prego, R., Valero-Garcés, B.L., Pueyo, J.J., González-Sampériz, P. & Taberner, C. (2008) A statistical approach to disentangle environmental forcings in a lacustrine record: the Lago Chungará case (Chilean Altiplano). *Journal of Paleolimnology*, 40, 195–215.

Giralt, S.R. (1998) El registre dels llacs salins con arxius paleoclimàtics: salines (alacant) i gallocanta (aragó). Universitat de Barcelona.

Guo, P., Wen, H., Li, C., He, H. & Sánchez-Román, M. (2023) Lacustrine dolomite in deep time: what really matters in early dolomite formation and accumulation? *Earth-Science Reviews*, 246, 104575.

Guo, P., Wen, H. & Sánchez-Román, M. (2023) Constraints on dolomite formation in a Late Palaeozoic saline alkaline lake deposit, Junggar Basin, north-west China. *Sedimentology*, 70, 2302–2330.

Held, F., Cheng, H., Edwards, R., Tüysüz, O., Koç, K. & Fleitmann, D. (2024) Dansgaard-Oeschger cycles of the penultimate and last glacial period recorded in stalagmites from Türkiye. *Nature Communications*, 15, 1183.

Helmi, F.M., Elmitwalli, H.R., Elnagdy, S.M. & El-Hagrassy, A.F. (2016) Calcium carbonate precipitation induced by ureolytic bacteria Bacillus licheniformis. *Ecological Engineering*, 90, 367–371.

Horton, T.W., Defliese, W.F., Tripati, A.K. & Oze, C. (2016) Evaporation induced 18O and 13C enrichment in lake systems: a global perspective on hydrologic balance effects. *Quaternary Science Reviews*, 131, 365–379.

Hudson, A.M., Quade, J., Ali, G., Boyle, D., Bassett, S., Huntington, K.W., Marie, G., Cohen, A.S., Lin, K. & Wang, X. (2017) Stable C, O and clumped isotope systematics and 14C geochronology of carbonates from the Quaternary Chewaucan closed-basin lake system, Great Basin, USA: implications for paleoenvironmental reconstructions using carbonates. *Geochimica et Cosmochimica Acta*, 212, 274–302.

Julià, R., Negendank, J., Seret, G., Brauer, A., Burjachs, F., Endres, C., Giralt, S., Parés, J. & Roca, J. (1994) Holocene climatic change and desertification in the Western Mediterranean region. *Terra Nostra*, 1, 81–84.

Katoh, K., Misawa, K., Kuma, K.I. & Miyata, T. (2002) MAFFT: a novel method for rapid multiple sequence alignment based on fast Fourier transform. *Nucleic Acids Research*, 30, 3059–3066.

Land, L.S. (1998) Failure to precipitate dolomite at 25 C from dilute solution despite 1000-fold oversaturation after32 years. *Aquatic Geochemistry*, 4, 361–368.

Li, P.-E., Lo, C.-C., Anderson, J.J., Davenport, K.W., Bishop-Lilly, K.A., Xu, Y., Ahmed, S., Feng, S., Mokashi, V.P. & Chain, P.S. (2017) Enabling the democratization of the genomics revolution with a fully integrated web-based bioinformatics platform. *Nucleic Acids Research*, 45, 67–80.

Lippmann, F. (1973) *Crystal chemistry of sedimentary carbonate minerals*. Berilin Heidelberg: Springer.

Liu, D., Fan, Q., Papineau, D., Yu, N., Chu, Y., Wang, H., Qiu, X. & Wang, X. (2020) Precipitation of protodolomite facilitated by sulfate-reducing bacteria: the role of capsule extracellular polymeric substances. *Chemical Geology*, 533, 119415.

Liu, D., Xu, Y., Papineau, D., Yu, N., Fan, Q., Qiu, X. & Wang, H. (2019) Experimental evidence for abiotic formation of low-temperature proto-dolomite facilitated by clay minerals. *Geochimica et Cosmochimica Acta*, 247, 83–95.

Liu, D., Xu, Y., Yu, Q., Yu, N., Qiu, X., Wang, H. & Papineau, D. (2020) Catalytic effect of microbially-derived carboxylic acids on the precipitation of Mg-calcite and disordered dolomite: implications for sedimentary dolomite formation. *Journal of Asian Earth Sciences*, 193, 104301.

Liu, D., Yu, N., Papineau, D., Fan, Q., Wang, H., Qiu, X., She, Z. & Luo, G. (2019) The catalytic role of planktonic aerobic heterotrophic bacteria in protodolomite formation: results from Lake Jibuhulangtu Nuur, Inner Mongolia, China. *Geochimica et Cosmochimica Acta*, 263, 31–49.

Liutkus, C.M. & Wright, J.D. (2008) The influence of hydrology and climate on the isotope geochemistry of playa carbonates: a study from Pilot Valley, NV, USA. *Sedimentology*, 55, 965–978.

Lloyd, R. (1966) Oxygen isotope enrichment of sea water by evaporation. *Geochimica et Cosmochimica Acta*, 30, 801–814.

Lougheed, B.C. & Obrochta, S.P. (2019) A rapid, deterministic age-depth modeling routine for geological sequences with inherent depth uncertainty. *Paleoceanography and Paleoclimatology*, 34(1), 122–133. https://doi.org/10.1029/2018pa003457

Ma, J., Wu, C., Wang, Y., Wang, J., Fang, Y., Zhu, W., Zhai, L. & Zhou, T. (2017) Paleoenvironmental reconstruction of a saline lake in the Tertiary: evidence from aragonite laminae in the northern Tibet Plateau. *Sedimentary Geology*, 353, 1–12.

Magny, M., Miramont, C. & Sivan, O. (2002) Assessment of the impact of climate and anthropogenic factors on Holocene Mediterranean vegetation in Europe on the basis of palaeohydrological records. *Palaeogeography, Palaeoclimatology, Palaeoecology*, 186, 47–59.

Marcott, S.A., Shakun, J.D., Clark, P.U. & Mix, A.C. (2013) A reconstruction of regional and global temperature for the past 11,300 years. *Science*, 339, 1198–1201.

McCormack, J., Baldermann, A., Bontognali, T.R., Wolf, A. & Kwiecien, O. (2024) Hydrochemical mixing-zones trigger dolomite formation in an alkaline lake. *Sedimentology*, 71, 871–886.

McCormack, J. & Kwiecien, O. (2021) Coeval primary and diagenetic carbonates in lacustrine sediments challenge palaeoclimate interpretations. *Scientific Reports*, 11, 7935.

McCormack, J., Nehrke, G., Jöns, N., Immenhauser, A. & Kwiecien, O. (2019) Refining the interpretation of lacustrine carbonate isotope records: implications of a mineralogy-specific Lake Van case study. *Chemical Geology*, 513, 167–183.

McKenzie, J.A. & Vasconcelos, C. (2009) Dolomite Mountains and the origin of the dolomite rock of which they mainly consist: historical developments and new perspectives. *Sedimentology*, 56, 205–219.

Meyers, P.A. & Lallier-Vergès, E. (1999) Lacustrine sedimentary organic matter records of Late Quaternary paleoclimates. *Journal of Paleolimnology*, 21, 345–372.

Miller, Q.R., Schaef, H.T., Kaszuba, J.P., Qiu, L., Bowden, M.E. & Mcgrail, B.P. (2018) Tunable manipulation of mineral carbonation kinetics in nanoscale water films via citrate additives. *Environmental Science & Technology*, 52, 7138–7148.

Morellon, M., Valero-Garces, B., Vegas-Vilarrubia, T., Gonzalez-Samperiz, P., Romero, O., Delgado-Huertas, A., Mata, P., Moreno, A., Rico, M. & Corella, J.P. (2009) Lateglacial and Holocene palaeohydrology in the western Mediterranean region: the Lake Estanya record (NE Spain). *Quaternary Science Reviews*, 28, 2582–2599.

Mueller, M., Jacquemyn, C., Walter, B.F., Pederson, C.L., Schurr, S.L., Igbokwe, O.A., Jöns, N., Riechelmann, S., Dietzel, M. & Strauss, H. (2022) Constraints on the preservation of proxy data in carbonate archives–lessons from a marine limestone to marble transect, Latemar, Italy. *Sedimentology*, 69, 423–460.

Naim, Z., Li, G., Gibert, L., Stuut, J., Jiménez-Moreno, G. & Sánchez-Román, M. (2025) Laguna Fuente de Piedra: an example of a dolomite factory recording ~50,000 years of depositional and paleoclimatic evolution. *The Depositional Record*. https://doi.org/10.1002/dep2.70052

Ninyerola, M., I Fernández, X.P. & Roure, J.M. (2005) *Atlas climático digital de la Península Ibérica*: *metodología y aplicaciones en bioclimatología y geobotánica*.

North Greenland Ice Core Project members. (2004) High-resolution record of Northern Hemisphere climate extending into the last interglacial period. *Nature*, 431(7005), 147–151. https://doi.org/10.1038/nature02805

Pepiol-Salom, E., Batlle-Sales, J. & Bordás-Valls, V. (1999) Geostatistic study of salt distribution in "laguna de Salinas". In: *geoENV II—Geostatistics for Environmental Applications: proceedings of the Second European Conference on Geostatistics for Environmental*

Applications held in Valencia, Spain, November 18–20, 1998. Alicante, Spain: Springer, pp. 441–452.

Petrash, D.A., Bialik, O.M., Bontognali, T.R., Vasconcelos, C., Roberts, J.A., McKenzie, J.A. & Konhauser, K.O. (2017) Microbially catalyzed dolomite formation: from near-surface to burial. *Earth-Science Reviews*, 171, 558–582.

Petrash, D.A., Lalonde, S.V., González-Arismendi, G., Gordon, R.A., Méndez, J.A., Gingras, M.K. & Konhauser, K.O. (2015) Can Mn–S redox cycling drive sedimentary dolomite formation? A hypothesis. *Chemical Geology*, 404, 27–40.

Pineda, V., Gibert, L., Soria, J.M., Carrazana, A., Ibáñez-Insa, J. & Sánchez-Román, M. (2021) Interevaporitic deposits of Las Minas gypsum unit: a record of late Tortonian marine incursions and dolomite precipitation in Las Minas basin (eastern betic Cordillera, SE Spain). *Palaeogeography, Palaeoclimatology, Palaeoecology*, 564, 110171.

Popall, R.M., Bolhuis, H., Muyzer, G. & Sánchez-Román, M. (2020) Stromatolites as biosignatures of atmospheric oxygenation: carbonate biomineralization and UV-C resilience in a geitlerinemasp.—dominated culture. *Frontiers in Microbiology*, 11, 948.

Power, I.M., Kenward, P.A., Dipple, G.M. & Raudsepp, M. (2017) Room temperature magnesite precipitation. *Crystal Growth & Design*, 17, 5652–5659.

Price, M.N., Dehal, P.S. & Arkin, A.P. (2009) FastTree: computing large minimum evolution trees with profiles instead of a distance matrix. *Molecular Biology and Evolution*, 26, 1641–1650.

Qiu, X., Wang, H., Yao, Y. & Duan, Y. (2017) High salinity facilitates dolomite precipitation mediated by Haloferax volcanii DS52. *Earth and Planetary Science Letters*, 472, 197–205.

Qiu, Z., Tao, H., Lu, B., Chen, Z., Wu, S., Liu, H. & Qiu, J. (2021) Controlling factors on organic matter accumulation of marine shale across the Ordovician-Silurian transition in South China: constraints from trace-element geochemistry. *Journal of Earth Science*, 32, 887–900.

Queralt, I., Querol, X., López-Soler, A. & Plana, F. (1997) Use of coal fly ash for ceramics: a case study for a large Spanish power station. *Fuel*, 76, 787–791.

Rigual, A. (1972) Flora y vegetación de la provincia de Alicante. *Instituto de Estudios alicantinos*, 2(1), 1–403.

Roberts, J.A., Kenward, P.A., Fowle, D.A., Goldstein, R.H., González, L.A. & Moore, D.S. (2013) Surface chemistry allows for abiotic precipitation of dolomite at low temperature. *Proceedings of the National Academy of Sciences of the United States of America*, 110, 14540–14545.

Roca, J.R. & Juliá, R. (1997) Late-glacial and Holocene lacustrine evolution based on ostracode assemblages in Southeastern Spain. *Geobios*, 30, 823–830.

Rognes, T., Flouri, T., Nichols, B., Quince, C. & Mahé, F. (2016) VSEARCH: a versatile open source tool for metagenomics. *PeerJ*, 4, e2584.

Rosen, M.R., Turner, J.V., Coshell, L. & Gailitis, V. (1995) The effects of water temperature, stratification, and biological activity on the stable isotopic composition and timing of carbonate precipitation in a hypersaline lake. *Geochimica et Cosmochimica Acta*, 59, 979–990.

Sánchez-Román, M., Chandra, V., Mulder, S., Areias, C., Reijmer, J. & Vahrenkamp, V. (2025) The hidden role of heterotrophic bacteria in early carbonate diagenesis. *Scientific Reports*, 15, 561.

Sánchez-Román, M., Fernández-Remolar, D., Amils, R., Sánchez-Navas, A., Schmid, T., Martin-Uriz, P.S., Rodríguez, N., McKenzie, J.A. & Vasconcelos, C. (2014) Microbial mediated formation of Fe-carbonate minerals under extreme acidic conditions. *Scientific Reports*, 4, 4767.

Sánchez-Román, M., Gibert, L., Martín-Martín, J.D., van Zuilen, K., Pineda-González, V., Vroon, P. & Bruggmann, S. (2023) Sabkha and salina dolomite preserves the biogeochemical conditions of its depositional paleoenvironment. *Geochimica et Cosmochimica Acta*, 356, 66–82.

Sánchez-Román, M., McKenzie, J.A., Wagener, A.D.L.R., Romanek, C.S., Sánchez-Navas, A. & Vasconcelos, C. (2011) Experimentally determined biomediated Sr partition coefficient for dolomite: significance and implication for natural dolomite. *Geochimica et Cosmochimica Acta*, 75, 887–904.

Sanchez-Roman, M., Puente-Sanchez, F., Parro, V. & Amils, R. (2015) Nucleation of Fe-rich phosphates and carbonates on microbial cells and exopolymeric substances. *Frontiers in Microbiology*, 6, 1024.

Sánchez-Román, M., Rivadeneyra, M.A., Vasconcelos, C. & McKenzie, J.A. (2007) Biomineralization of carbonate and phosphate by moderately halophilic bacteria. *FEMS Microbiology Ecology*, 61, 273–284.

Sánchez-Román, M., Romanek, C.S., Fernández-Remolar, D.C., Sánchez-Navas, A., McKenzie, J.A., Amils Pibernat, R. & Vasconcelos, C. (2011) Aerobic biomineralization of Mg-rich carbonates: implications for natural environments. *Chemical Geology*, 281, 143–150.

Sánchez-Román, M., Vasconcelos, C., Schmid, T., Dittrich, M., McKenzie, J.A., Zenobi, R. & Rivadeneyra, M.A. (2008) Aerobic microbial dolomite at the nanometer scale: implications for the geologic record. *Geology*, 36, 879–882.

Sánchez-Román, M., Vasconcelos, C., Warthmann, R., Rivadeneyra, M. & McKenzie, J.A. (2009) Microbial dolomite precipitation under aerobic conditions: results from Brejo do Espinho Lagoon (Brazil) and culture experiments. In: *Perspectives in carbonate geology: a tribute to the career of Robert Nathan Ginsburg*, pp. 167–178. https://doi.org/10.1002/9781444312065.ch11

Schannwell, C., Mikolajewicz, U., Kapsch, M.-L. & Ziemen, F. (2024) A mechanism for reconciling the synchronisation of Heinrich events and Dansgaard-Oeschger cycles. *Nature Communications*, 15(1), 2961. https://doi.org/10.1038/s41467-024-47141-7

Singer, B.S., Guillou, H., Jicha, B.R., Zanella, E. & Camps, P. (2014) Refining the Quaternary geomagnetic instability time scale (GITS): lava flow recordings of the Blake and Post-Blake excursions. *Quaternary Geochronology*, 21, 16–28.

Talbot, M. (1990) A review of the palaeohydrological interpretation of carbon and oxygen isotopic ratios in primary lacustrine carbonates. *Chemical Geology: Isotope Geoscience Section*, 80, 261–279.

Valero-Garcés, B., Morellón, M., Moreno, A., Corella, J.P., Martín-Puertas, C., Barreiro, F., Pérez, A., Giralt, S. & Mata-Campo, M.P. (2014) Lacustrine carbonates of Iberian Karst Lakes: sources, processes and depositional environments. *Sedimentary Geology*, 299, 1–29.

Valero-Garcés, B.L., González-Sampériz, P., Navas, A., MACHíN, J., Delgado-Huertas, A., Peña-Monné, J.L., Sancho-Marcén, C., Stevenson, T. & Davis, B. (2004) Paleohydrological fluctuations and steppe vegetation during the last glacial maximum in the central Ebro valley (NE Spain). *Quaternary International*, 122, 43–55.

van Lith, Y., Warthmann, R., Vasconcelos, C. & McKenzie, J.A. (2003) Sulphate-reducing bacteria induce low-temperature Ca-dolomite and high Mg-calcite formation. *Geobiology*, 1, 71–79.

Vasconcelos, C. & McKenzie, J.A. (1997) Microbial mediation of modern dolomite precipitation and diagenesis under anoxic conditions (Lagoa Vermelha, Rio de Janeiro, Brazil). *Journal of Sedimentary Research*, 67, 378–390.

Vasconcelos, C., McKenzie, J.A., Warthmann, R. & Bernasconi, S.M. (2005) Calibration of the δ18O paleothermometer for dolomite precipitated in microbial cultures and natural environments. *Geology*, 33(4), 317. https://doi.org/10.1130/g20992.1

Vos, P., Garrity, G., Jones, D., Krieg, N.R., Ludwig, W., Rainey, F.A., Schleifer, K.-H. & Whitman, W.B. (2011) *Bergey's manual of systematic bacteriology: volume 3: the Firmicutes*. Springer Science & Business Media.

Wacey, D., Wright, D.T. & Boyce, A.J. (2007) A stable isotope study of microbial dolomite formation in the Coorong Region, South Australia. *Chemical Geology*, 244, 155–174.

Wanas, H. & Sallam, E. (2016) Abiotically-formed, primary dolomite in the mid-Eocene lacustrine succession at Gebel El-Goza El-Hamra, NE Egypt: an approach to the role of smectitic clays. *Sedimentary Geology*, 343, 132–140.

Wang, Y., Wu, C., Fang, Y., Ma, J., Shen, B., Huang, F., Li, L., Ning, M., Zhai, L. & Zhang, W. (2020) Mg, C and O isotopic compositions of Late Cretaceous lacustrine dolomite and travertine in the northern Tianshan Mountains, Northwest China. *Chemical Geology*, 541, 119569.

Warren, J. (2000) Dolomite: occurrence, evolution and economically important associations. *Earth-Science Reviews*, 52, 1–81.

Wen, Y., Sánchez-Román, M., Li, Y., Wang, C., Han, Z., Zhang, L. & Gao, Y. (2020) Nucleation and stabilization of Eocene dolomite in evaporative lacustrine deposits from central Tibetan plateau. *Sedimentology*, 67, 3333–3354.

Wright, D.T. (1999) The role of sulphate-reducing bacteria and cyanobacteria in dolomite formation in distal ephemeral lakes of the Coorong region, South Australia. *Sedimentary Geology*, 126, 147–157.

Wright, D.T. & Wacey, D. (2005) Precipitation of dolomite using sulphate-reducing bacteria from the Coorong Region, South Australia: significance and implications. *Sedimentology*, 52, 987–1008.

Yao, T., Zhu, H., Fu, B., Xiaofeng, D., Wang, O., Sen, L., Yang, X. & Sánchez-Román, M. (2024) Origin of Eocene lacustrine dolomite and evolution of multiple diagenetic fluids in the Huanghekou sag, Bohai Bay Basin. *AAPG Bulletin*, 108, 1957–1984.

Zhao, Y., Wei, X., Han, Z., Han, C., Gao, X., Meng, R., Wang, Q., Tucker, M.E., Li, M. & Sánchez-Román, M. (2023) Lacustrine-evaporitic microbial dolomite from a Plio-Pleistocene succession recovered by the SG-1 borehole in the Qaidam Basin, NE Tibetan Plateau. *Chemical Geology*, 622, 121376.

SUPPORTING INFORMATION

Additional supporting information can be found online in the Supporting Information section at the end of this article.

How to cite this article: Li, G., Naim, Z., Gibert, L., Stuut, J.-B., Waajen, A.C., Jimenez-Moreno, G. et al. (2026) Microbial mediation and climatic control on dolomite precipitation in a hypersaline lake: Insights from Salinas Lake, southern Iberia. *The Depositional Record*, 12, e70058. Available from: https://doi.org/10.1002/dep2.70058